Available online at www.sciencedirect.com
SCIENCE DIRECT®
Comput. Methods Appl. Mech. Engrg. 192 (2003) 3933–3957
Computer methods in applied mechanics and engineering
www.elsevier.com/locate/cma

Voronoi-based finite volume methods, optimal Voronoi meshes, and PDEs on the sphere ☆

Qiang Du [a,1], Max D. Gunzburger [b,*], Lili Ju [c]

[a] Department of Mathematics, Pennsylvania State University, University Park, PA 16802, USA
[b] School of Computational Science and Information Technology, Florida State University, Tallahassee, FL 32306-4120, USA
[c] Institute for Mathematics and its Applications, University of Minnesota, Minneapolis, MN 55455, USA

Received 8 July 2002; received in revised form 6 May 2003; accepted 7 May 2003

Abstract

We first develop and analyze a finite volume scheme for the discretization of partial differential equations (PDEs) on the sphere; the scheme uses Voronoi tessellations of the sphere. For a model convection–diffusion problem, the finite volume scheme is shown to produce first-order accurate approximations with respect to a mesh-dependent discrete first-derivative norm. Then, we introduce the notion of constrained centroidal Voronoi tessellations (CCVTs) of the sphere; these are special Voronoi tessellation of the sphere for which the generators of the Voronoi cells are also the constrained centers of mass, with respect to a prescribed density function, of the cells. After discussing an algorithm for determining CCVT meshes on the sphere, we discuss and illustrate several desirable properties possessed by these meshes. In particular, it is shown that CCVT meshes define very high-quality uniform and non-uniform meshes on the sphere. Finally, we discuss, through some computational experiments, the performance of the CCVT meshes used in conjunction with the finite volume scheme for the solution of simple model PDEs on the sphere. The experiments show, for example, that the CCVT based finite volume approximations are second-order accurate if errors are measured in discrete L^2 norms.

1. Introduction

Much effort has been devoted to finite element methods or mixed finite element methods for solving partial differential equations on the sphere and other surfaces. One approach [2] is to construct finite element basis functions based on spherical triangles and then discretize the differential equations exactly as in standard finite element methods. Another approach [9] is to approximate the sphere (or a more general surface) by a polyhedron which consists of the union of planar triangles, and then assemble the Galerkin

☆ Supported by the National Science Foundation under grant number CCR-9988303.
* Corresponding author.
E-mail addresses: qdu@math.psu.edu (Q. Du), gunzburg@csit.fsu.edu (M.D. Gunzburger), ju@ima.umn.edu (L. Ju).
[1] The work of this author was also supported in part by NSF DMS-0196522 and NSF ITR-0205232.

0045-7825/$ - see front matter © 2003 Elsevier B.V. All rights reserved.
doi:10.1016/S0045-7825(03)00394-3

equations with respect to these triangles by projection. Both approaches have almost the same convergence properties that are also the same as those for standard finite element methods in the plane.

Finite difference methods are less effective for many problems posed on the sphere due to the difficulty of constructing higher-order approximation of surface derivatives.

Finite volume methods for general domains in $\mathbb{R}^d$ ($d = 2, 3$) have been broadly used in various practical applications and also studied theoretically [8,10,15,16,21,22]. They are well regarded for the discretization of conservation equations with convection terms. The stability and convergence have been studied in [3,12,15,19,20,22]. The available theory are generally based on either estimates in some discrete norms or by viewing a finite volume method as a mixed finite element method [21]. However, fewer efforts have been specifically directed at constructing and analyzing finite volume methods on the sphere which may be of particular interest in many applications including oceanic and atmospheric modeling.

Finite volume methods based on Voronoi meshes [1] in the plane are widely used in engineering applications. In [4,10,16], error estimates were proved that show that approximations are at least first-order accurate with respect to discrete L^p ($p \geqslant 2$) and H^1 norms; numerical experiments, however, indicated second-order convergence rates with respect to a discrete L^2 norm [16]. In the context of other discretization methods, Voronoi meshes as well as their dual meshes (Delaunay triangulations) are very popular and are well suited for gridding the sphere.

The first goal of this paper is to construct and analyze a Voronoi-based finite volume method for determining approximate solutions of a model convection–diffusion problem that is defined in Section 1.1. First, Voronoi meshes on the sphere are discussed in Section 2; it turns out that the concept of Delaunay triangulation and Voronoi tessellation can be extended to the surface of sphere in a natural way [18]. Then, a finite volume discretization scheme for the model partial differential equations is constructed (in Section 3) and analyzed (in Section 4). The second goal of this paper is to present a class of special Voronoi meshes on the sphere based on the concept of *constrained centroidal Voronoi tessellations* (CCVTs) [6]. These special tessellations of the sphere can be shown to be optimal in some sense. Section 5 is devoted to a discussion of the construction of CCVTs on the sphere and of their desirable properties. In Section 6, the results of some computational experiments are presented. Finally, in Section 7, some concluding remarks are provided.

The Delaunay dual mesh corresponding to a CCVT can also be very useful, in the context of finite element methods, for computations on the sphere. This use of CCVTs will be discussed in our future works.

1.1. Preliminaries

Let $\mathbf{S}^2$ denote the (surface of the) sphere having radius $r > 0$, i.e.,

$$\mathbf{S}^2 = \left\{\mathbf{x} = (x_1, x_2, x_3) \in \mathbb{R}^3 \,|\, \|\mathbf{x}\| = r\right\},$$

where $\|\cdot\|$ denotes the Euclidean norm. (Throughout the paper, "sphere" will denote the surface of a ball in $\mathbb{R}^3$.) Let ∇_s denote the tangential gradient operator [9,11] on $\mathbf{S}^2$ defined by

$$\nabla_s u(\mathbf{x}) = (\nabla_{s,1}, \nabla_{s,2}, \nabla_{s,3})u(\mathbf{x}) = \nabla u(\mathbf{x}) - (\nabla u(\mathbf{x}) \cdot \vec{\mathbf{n}}_{\mathbf{S}^2,\mathbf{x}})\vec{\mathbf{n}}_{\mathbf{S}^2,\mathbf{x}},$$

where $\nabla = (D_1, D_2, D_3)$ denotes the general gradient operator in $\mathbb{R}^3$ and $\vec{\mathbf{n}}_{\mathbf{S}^2,\mathbf{x}}$ is the outer normal vector to $\mathbf{S}^2$ at $\mathbf{x}$. We consider the *convection–diffusion problem on the sphere* governed by

$$\nabla_s \cdot \Big(- a(\mathbf{x})\nabla_s u(\mathbf{x}) + \vec{\mathbf{v}}(\mathbf{x})u(\mathbf{x})\Big) + b(\mathbf{x})u(\mathbf{x}) = f(\mathbf{x}) \quad \text{for } \mathbf{x} \in \mathbf{S}^2. \tag{1.1}$$

Note that, since $\mathbf{S}^2$ has no boundary, there is no boundary condition imposed.

We use the standard notation for Sobolev spaces on $\mathbf{S}^2$ (a compact, two-dimensional Riemannian manifold) [11]:

$$L^p(\mathbf{S}^2) = \left\{ u(\mathbf{x}) \,\middle|\, \int_{\mathbf{S}^2} |u(\mathbf{x})|^p \, \mathrm{d}s(\mathbf{x}) < \infty \right\},$$

$$W^{m,p}(\mathbf{S}^2) = \left\{ u \in L^2(\mathbf{S}^2) \,|\, \nabla_s^\alpha u \in L^p(\mathbf{S}^2) \quad \text{for } 0 \leqslant |\alpha| \leqslant m \right\},$$

where $\alpha = (\alpha_1, \alpha_2, \alpha_3)$, $\nabla_s^\alpha = \nabla_{s,1}^{\alpha_1} \nabla_{s,2}^{\alpha_2} \nabla_{s,3}^{\alpha_3}$, and $|\alpha| = \alpha_1 + \alpha_2 + \alpha_3$. A norm for $W^{m,p}(\mathbf{S}^2)$ is defined by

$$\|u\|_{W^{m,p}(\mathbf{S}^2)} = \begin{cases} \left(\sum_{0 \leqslant |\alpha| \leqslant m} \|\nabla_s^\alpha u\|_{L^p(\mathbf{S}^2)}^p \right)^{1/p} & \text{for } 1 \leqslant p < \infty, \\ \max_{0 \leqslant |\alpha| \leqslant m} \|\nabla_s^\alpha u\|_{L^\infty(\mathbf{S}^2)} & \text{for } p = \infty. \end{cases}$$

Let $H^m(\mathbf{S}^2) = W^{m,2}(\mathbf{S}^2)$.

We assume that the data in (1.1) satisfy the following set of assumptions.

Assumption 1. $f \in L^2(\mathbf{S}^2)$, $a \in C^1(\mathbf{S}^2)$, $b \in L^\infty(\mathbf{S}^2)$, and $\vec{\mathbf{v}} \in C^1(\mathbf{S}^2, \mathbb{R}^3)$ such that $a(\mathbf{x}) \geqslant \alpha_1 > 0$, $b(\mathbf{x}) \geqslant 0$, and $\nabla_s \cdot \vec{\mathbf{v}}(\mathbf{x}) + b(\mathbf{x}) \geqslant \alpha_2 > 0$, a.e.

Since $\mathbf{S}^2$ is compact, if Assumption 1 holds the problem (1.1) has a unique solution $u \in H^2(\mathbf{S}^2)$ that satisfies (for some constant $C > 0$) the estimate

$$\|u\|_{H^2(\mathbf{S}^2)} \leqslant C \|f\|_{L^2(\mathbf{S}^2)} \tag{1.2}$$

and

$$\int_{\mathbf{S}^2} b(\mathbf{x}) u(\mathbf{x}) \, \mathrm{d}s(\mathbf{x}) = \int_{\mathbf{S}^2} f(\mathbf{x}) \, \mathrm{d}s(\mathbf{x}) \quad \text{and} \quad \int_{\mathbf{S}^2} \mathscr{L} u(\mathbf{x}) \, \mathrm{d}s(\mathbf{x}) = 0, \tag{1.3}$$

where $\mathscr{L} u = \nabla_s \cdot (-a \nabla_s u + \vec{\mathbf{v}} u)$.

2. Voronoi meshes on the sphere and discrete norms

Denote by $\mathrm{d}(\mathbf{x}, \mathbf{y})$ the geodesic distance between $\mathbf{x}$ and $\mathbf{y}$ on $\mathbf{S}^2$, i.e.,

$$\mathrm{d}(\mathbf{x}, \mathbf{y}) = r \left[\arccos \left(\frac{\mathbf{x} \cdot \mathbf{y}}{r^2} \right) \right] \quad \text{for } \mathbf{x}, \mathbf{y} \in \mathbf{S}^2.$$

Given a set of distinct points $\{\mathbf{x}_i\}_{i=1}^n \subset \mathbf{S}^2$, we can define for each point $\mathbf{x}_i$, $i = 1, \ldots, n$, the corresponding Voronoi region V_i, $i = 1, \ldots, n$, by

$$V_i = \left\{ \mathbf{y} \in \mathbf{S}^2 \,|\, \mathrm{d}(\mathbf{x}_i, \mathbf{y}) < \mathrm{d}(\mathbf{x}_j, \mathbf{y}) \quad \text{for } j = 1, \ldots, n \text{ and } j \neq i \right\}.$$

Clearly, we have $\mathbf{x}_i \in V_i$, $V_i \cap V_j = \emptyset$ for $i \neq j$, and $\cup_{i=1}^n \overline{V}_i = \mathbf{S}^2$ so that $\{V_i\}_{i=1}^n$ is a tessellation of $\mathbf{S}^2$. We refer to $\{V_i\}_{i=1}^n$ as the *Voronoi tessellation* or *Voronoi diagram* of $\mathbf{S}^2$ associated with the point set $\{\mathbf{x}_i\}_{i=1}^n$. A point $\mathbf{x}_i$ is called a *generator*; a subdomain $V_i \subset \mathbf{S}^2$ is referred to as the *Voronoi region* or *Voronoi cell* corresponding to the generator $\mathbf{x}_i$. It is easy to see that each Voronoi cell V_i is an open convex spherical polygon on $\mathbf{S}^2$, i.e., its sides are geodesic arcs. It is also well-known that the dual tessellation (in a graph-theoretical sense) to a Voronoi tessellation of $\mathbf{S}^2$ consists of spherical triangles. The dual tessellations are referred to as *Delaunay triangulations* and are very popular computational meshes on the sphere. Algorithms for the construction of Voronoi diagrams and Delaunay triangulations on the sphere are discussed in [18].

We refer to any pair of generators $\mathbf{x}_i$ and $\mathbf{x}_j$ as *neighbors* if and only if $\Gamma_{ij} = \overline{V}_i \cap \overline{V}_j \neq \emptyset$. Note that, for Voronoi meshes, Γ_{ij} can only be a point or a geodesic arc on the sphere. Let

$$m(A) = \begin{cases} \text{the area of } A \text{ if it is a non-empty subdomain of } \mathbf{S}^2, \\ \text{the length of } A \text{ if it is a geodesic arc on } \mathbf{S}^2. \end{cases}$$

Then, for each $\mathbf{x}_i$, we denote by χ_i the set of the indices of its neighbors $\mathbf{x}_j$'s such that $m(\Gamma_{ij}) > 0$, i.e., of those neighbors for which Γ_{ij} is a geodesic arc. We also denote by $\overline{\mathbf{x}_i\mathbf{x}_j}$ the vector from $\mathbf{x}_i$ to $\mathbf{x}_j$, by $\widetilde{\mathbf{x}_i\mathbf{x}_j}$ the geodesic arc joining $\mathbf{x}_i$ and $\mathbf{x}_j$, and by $\mathbf{x}_{ij}$ the midpoint of the geodesic arc $\widetilde{\mathbf{x}_i\mathbf{x}_j}$. By the construction of Voronoi tessellations, it is known that $\widetilde{\mathbf{x}_i\mathbf{x}_j}$ is perpendicular to Γ_{ij} and the plane determined by Γ_{ij} and the origin bisects $\widetilde{\mathbf{x}_i\mathbf{x}_j}$ at its midpoint $\mathbf{x}_{ij}$ [18]; see Fig. 1. Thus, we have

$$\mathrm{d}(\mathbf{x}_i, \mathbf{x}) = \mathrm{d}(\mathbf{x}_j, \mathbf{x}) \quad \text{and} \quad \vec{\mathbf{n}}_{\mathbf{x},V_k} \| \overline{\mathbf{x}_i\mathbf{x}_j} \quad \text{for } \mathbf{x} \in \Gamma_{ij}, \ \ k = i, j, \tag{2.1}$$

where $\vec{\mathbf{n}}_{\mathbf{x},V_i}$ is the outer unit normal vector at the boundary point $\mathbf{x}$ of V_i lying in the surface tangent to $\mathbf{S}^2$ at $\mathbf{x}$.

A function u defined on $\mathbf{S}^2$ is called a *grid function* associated with a mesh $\mathscr{W} = \{\mathbf{x}_i, V_i\}_{i=1}^n$ if $u(\mathbf{x}) = u(\mathbf{x}_i)$ for all $\mathbf{x} \in V_i$, i.e., $u(\mathbf{x})$ is constant on each cell V_i. For given grid functions u, v on $\mathbf{S}^2$, we define, similar to [16], the following discrete inner products and norms associated with a mesh $\mathscr{W} = \{\mathbf{x}_i, V_i\}_{i=1}^n$:

$$\begin{cases} (u, v) = \sum_{i=1}^n m(V_i) u(\mathbf{x}_i) v(\mathbf{x}_i), \quad \|u\|_{0,\mathscr{W}}^2 = (u, u), \\ |u|_{1,\mathscr{W}}^2 = \frac{1}{2} \sum_{i=1}^m \sum_{j \in \chi_i} m(\Gamma_{ij}) \, \mathrm{d}(\mathbf{x}_i, \mathbf{x}_j) \left(\dfrac{u(\mathbf{x}_i) - u(\mathbf{x}_j)}{\|\mathbf{x}_i - \mathbf{x}_j\|} \right)^2, \\ \|u\|_{1,\mathscr{W}}^2 = \|u\|_{0,\mathscr{W}}^2 + |u|_{1,\mathscr{W}}^2, \quad \text{and} \quad \|u\|_{-1,\mathscr{W}} = \sup_{\|v\|_{1,\mathscr{W}} \neq 0} \dfrac{|(u, v)|}{\|v\|_{1,\mathscr{W}}}. \end{cases}$$

We define the *mesh norm* h by

$$h = \max_{i=1,\ldots,n} h_i, \quad \text{where} \quad h_i = \max_{\mathbf{y} \in V_i} \mathrm{d}(\mathbf{x}_i, \mathbf{y}).$$

Thus, h_i gives the maximum geodesic distance between the particular generator $\mathbf{x}_i$ and the points in its associated cell V_i and h gives the maximum geodesic distance between any generator and the points in its associated cell. It is, of course, topologically impossible for the sphere $\mathbf{S}^2$ to be tessellated into a uniform

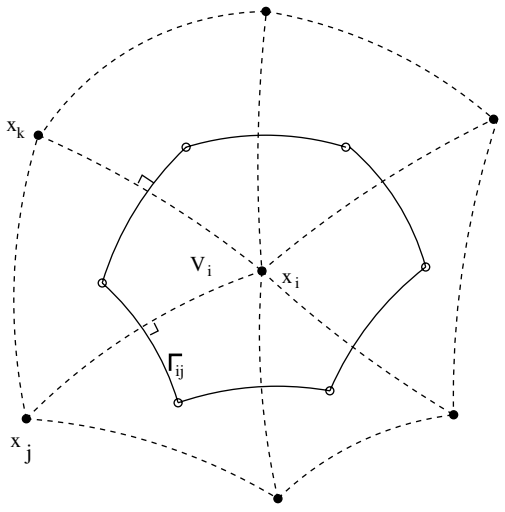

Fig. 1. A spherical Voronoi region.

mesh of, e.g., congruent hexagons. The mesh norm h can be used as a measure of the uniformity of mesh, i.e., of how "close" a mesh on $\mathbf{S}^2$ is to an ideal (and non-attainable) uniform mesh; the smaller the value of h, the more uniform is the mesh. The mesh norm h was used in this manner in [6] in the context of polynomial interpolation on the sphere.

Given a Voronoi finite volume mesh $\mathscr{W} = \{\mathbf{x}_i, V_i\}_{i=1}^m$, we define the *regularity norm* σ by

$$\sigma = \min_{i=1,\ldots,n} \sigma_i, \quad \text{where } \sigma_i = \min_{j\in\chi_i} \sigma_{ij} \quad \text{and} \quad \sigma_{ij} = \frac{\mathrm{d}(\mathbf{x}_i, \mathbf{x}_j)}{2h_i}. \tag{2.2}$$

To determine σ_{ij}, one computes, for the cell V_i, the ratio of half the distance between its generator $\mathbf{x}_i$ and one of its neighbor $\mathbf{x}_j$ and the maximum distance between the generator and the points in its cell, where distances are measured along geodesics. One then determines σ_i by minimizing σ_{ij} over the set of all neighbors of $\mathbf{x}_i$, i.e., over $j \in \chi_i$. Finally, σ is determined by minimizing σ_i over all cells, i.e., over $i = 1, \ldots, n$. For an ideal (and non-attainable) uniform mesh, $\sigma = \sigma_i = \sigma_{ij}$ for all i and j; any deviation from uniformity will reduce the value of σ. Thus, σ can be used as another measure of the uniformity of a mesh; the larger the value of σ, the more uniform is the mesh. In addition, the value of σ provides us a measure of the mesh regularity, i.e., the *local uniformity* of a mesh. Again, if a mesh is locally uniform in the sense that the cells in a neighborhood of any cell are nearly congruent to that cell, then the value of σ will again be large. We will refer to $\mathscr{W}$ as *regular* if σ is not "too small."

Meshes of the type $\mathscr{W} = \{\mathbf{x}_i, V_i\}_{i=1}^n$, where a V_i is the Voronoi region corresponding to the point $\mathbf{x}_i$, will be used as control (or finite) volumes for the discretization method discussed in Section 3; clearly, they are cell-centered meshes on $\mathbf{S}^2$. In order to obtain a reasonable theory and approximations, we will need to require a regularity condition on the mesh.

3. A finite volume discretization scheme

We seek an approximate solution of (1.1) in terms of grid functions defined with respect to a Voronoi mesh $\mathscr{W} = \{\mathbf{x}_i, V_i\}_{i=1}^n$. We denote the approximate solution by $u_i^h = u^h|_{V_i} = u(\mathbf{x}_i)$ for $i = 1, \ldots, n$. By Green's formula, we have

$$\int_{\partial V_i} (-a(\mathbf{x})\nabla_s u(\mathbf{x}) + \vec{\mathbf{v}}(\mathbf{x})u(\mathbf{x})) \cdot \vec{\mathbf{n}}_{\mathbf{x},V_i}\, \mathrm{d}\gamma(\mathbf{x}) + \int_{V_i} b(\mathbf{x})u(\mathbf{x})\, \mathrm{d}s(\mathbf{x}) = \int_{V_i} f(\mathbf{x})\, \mathrm{d}s(\mathbf{x}).$$

Since $\partial V_i = \cup_{j\in\chi_i} \Gamma_{ij}$, we have

$$\sum_{j\in\chi_i} \left(\int_{\Gamma_{ij}} (-a(\mathbf{x})\nabla_s u(\mathbf{x})) \cdot \vec{\mathbf{n}}_{\mathbf{x},V_i}\, \mathrm{d}\gamma(\mathbf{x}) + \int_{\Gamma_{ij}} (\vec{\mathbf{v}}(\mathbf{x})u(\mathbf{x})) \cdot \vec{\mathbf{n}}_{\mathbf{x},V_i}\, \mathrm{d}\gamma(\mathbf{x}) \right) + \int_{V_i} b(\mathbf{x})u(\mathbf{x})\, \mathrm{d}s(\mathbf{x}) = \int_{V_i} f(\mathbf{x})\, \mathrm{d}s(\mathbf{x}).$$

Denote by $\mathscr{F}_{ij}$ the approximate diffusion flux defined by

$$\mathscr{F}_{ij} = -m(\Gamma_{ij})a_{ij}\frac{u_j^h - u_i^h}{\|\mathbf{x}_j - \mathbf{x}_i\|} \approx \int_{\Gamma_{ij}} (-a(\mathbf{x})\nabla_s u(\mathbf{x})) \cdot \vec{\mathbf{n}}_{\mathbf{x},V_i}\, \mathrm{d}\gamma(\mathbf{x}), \tag{3.1}$$

where

$$a_{ij} = \frac{1}{m(\Gamma_{ij})} \int_{\Gamma_{ij}} a(\mathbf{x})\, \mathrm{d}\gamma(\mathbf{x}).$$

An approximate convection flux $\mathscr{V}_{ij}$ which leads to an up-wind scheme is defined by [13]

$$\mathscr{V}_{ij} = \beta_{ij}^{+} u_i^h + \beta_{ij}^{-} u_j^h \approx \int_{\Gamma_{ij}} (\vec{\mathbf{v}}(\mathbf{x}) u(\mathbf{x})) \cdot \vec{\mathbf{n}}_{\mathbf{x},V_i} \, \mathrm{d}\gamma(\mathbf{x}), \tag{3.2}$$

where

$$\beta_{ij}^{+} = \tfrac{1}{2}(\beta_{ij} + |\beta_{ij}|) \quad \text{and} \quad \beta_{ij}^{-} = \tfrac{1}{2}(\beta_{ij} - |\beta_{ij}|)$$

with

$$\beta_{ij} = \int_{\Gamma_{ij}} \vec{\mathbf{v}}(\mathbf{x}) \cdot \vec{\mathbf{n}}_{\mathbf{x},V_i} \, \mathrm{d}\gamma(\mathbf{x}).$$

For all V_i, let f_i and b_i respectively denote the mean value of f and b on V_i, i.e.,

$$f_i = \frac{1}{m(V_i)} \int_{V_i} f(x) \, \mathrm{d}s(\mathbf{x}) \quad \text{and} \quad b_i = \frac{1}{m(V_i)} \int_{V_i} b(x) \, \mathrm{d}s(\mathbf{x}). \tag{3.3}$$

Using the notations we have introduced, the finite volume scheme we consider is defined by the following system:

$$\sum_{j \in \chi_i} (\mathscr{F}_{ij} + \mathscr{V}_{ij}) + m(V_i) b_i u_i^h = m(V_i) f_i \quad \text{for } i = 1, \ldots, n. \tag{3.4}$$

Scaling (3.4) by $1/m(V_i)$ results in

$$(\mathscr{L}^h u^h)_i = \frac{1}{m(V_i)} \sum_{j \in \chi_i} (\mathscr{F}_{ij} + \mathscr{V}_{ij}) + b_i u_i^h = f_i \quad \text{for } i = 1, \ldots, n. \tag{3.5}$$

It is clear that the above scheme satisfies the discrete conservation law since

$$\sum_{i=1}^{n} \sum_{j \in \chi_i} (\mathscr{F}_{ij} + \mathscr{V}_{ij}) = 0$$

which follows from $\mathscr{F}_{ij} = -\mathscr{F}_{ji}$ and $\mathscr{V}_{ij} = -\mathscr{V}_{ji}$ if $\mathbf{x}_i$ and $\mathbf{x}_j$ are neighbors with $m(\Gamma_{ij}) > 0$.

Remark 1. An approximate convection flux may be defined for a central difference scheme by

$$\mathscr{V}_{ij} = \frac{\beta_{ij}}{2}(u_i^h + u_j^h). \tag{3.6}$$

Then, a stability condition such as

$$P_i = \max_{j \in \chi_i} \frac{|\beta_{ij}| \cdot \|\mathbf{x}_i - \mathbf{x}_j\|}{2m(\Gamma_{ij}) a_{ij}} \leqslant 1 \quad \text{for } i = 1, \ldots, n$$

is needed, where P_i is called the local Peclet number [13,16].

We also have the following discrete maximum principle.

Proposition 1. *Suppose that Assumption* 1 *is satisfied. Let* $\mathscr{F}_{ij}$, $\mathscr{V}_{ij}$, *and* b_i *be defined by* (3.1)–(3.3). *If* $L^h u^h > 0$ (*in the point-wise sense*), *then* $u^h > 0$.

Proof. Let $L_h = (l_{ij})$. It is clear that $a_{ij} \geqslant \alpha_1 > 0$, $\beta_{ij}^{+} \geqslant \max(\beta_{ij}, 0)$, $\beta_{ij}^{-} \leqslant \min(\beta_{ij}, 0)$, and

$$\frac{1}{m(V_i)}\sum_{j\in\chi_i}\beta_{ij}+b_i=\frac{1}{m(V_i)}\left(\sum_{j\in\chi_i}\int_{\Gamma_{ij}}\vec{\mathbf{v}}(\mathbf{x})\cdot\vec{\mathbf{n}}_{\mathbf{x},V_i}\,\mathrm{d}\gamma(\mathbf{x})+\int_{V_i}b(x)\,\mathrm{d}s(\mathbf{x})\right)$$
$$=\frac{1}{m(V_i)}\left(\int_{V_i}\nabla_s\cdot\vec{\mathbf{v}}(\mathbf{x})+b(\mathbf{x})\,\mathrm{d}s(\mathbf{x})\right)\geqslant\alpha_2>0$$

so that we have that

$$l_{ii}=\frac{1}{m(V_i)}\sum_{j\in\chi_i}\left(\frac{m(\Gamma_{ij})a_{ij}}{\|\mathbf{x}_j-\mathbf{x}_i\|}+\beta_{ij}^{+}\right)+b_i\geqslant\frac{1}{m(V_i)}\sum_{j\in\chi_i}\beta_{ij}+b_i>0$$

and

$$l_{ij}=\frac{1}{m(V_i)}\left(-\frac{m(\Gamma_{ij})a_{ij}}{\|\mathbf{x}_j-\mathbf{x}_i\|}+\beta_{ij}^{-}\right)<0\quad\text{for } j\neq i.$$

Additionally,

$$l_{ii}+\sum_{j\in\sigma_i}l_{ij}=\frac{1}{m(V_i)}\sum_{j\in\chi_i}(\beta_{ij}^{+}+\beta_{ij}^{-})+b_i=\frac{1}{m(V_i)}\sum_{j\in\chi_i}\beta_{ij}+b_i\geqslant\alpha_2>0.$$

Thus, L^h is an M-matrix which implies that $u^h=(L^h)^{-1}(f_1,\ldots,f_m)^{\mathrm{T}}>0$. □

Corollary 1. *The discrete system* (3.5) *has a unique solution.*

Proof. The result follows directly from Proposition 1. □

Additionally, L^h can be shown to be a coercive operator.

Proposition 2. *Suppose that Assumption* 1 *is satisfied. Let* $\mathscr{F}_{ij}$, $\mathscr{V}_{ij}$, *and* b_i *be defined by* (3.1)–(3.3). *Then, there exists a constant* $C>0$ *such that*

$$(L^hv,v)\geqslant C\|v\|_{1,\mathscr{W}}^2$$

for any grid function v *defined on* $\mathbf{S}^2$ *associated with* $\mathscr{W}=\{\mathbf{x}_i,V_i\}_{i=1}^n$.

Proof. Let $v(\mathbf{x})$ be a grid function defined on $\mathbf{S}^2$ and $v_i=v(\mathbf{x}_i)$. Then,

$$(L^hv,v)=I_1+I_2,$$

where

$$I_1=-\sum_{i=1}^{n}\sum_{j\in\chi_i}m(\Gamma_{ij})a_{ij}\frac{(v_j-v_i)}{\|\mathbf{x}_j-\mathbf{x}_i\|}v_i$$

and

$$I_2=\sum_{i=1}^{n}\sum_{j\in\chi_i}(\beta_{ij}^{+}v_i+\beta_{ij}^{-}v_j)v_i+\sum_{i=1}^{n}m(V_i)b_iv_i^2.$$

We can simplify I_1 by

$$I_1=\frac{1}{2}\sum_{i=1}^{n}\sum_{j\in\chi_i}\frac{m(\Gamma_{ij})a_{ij}}{\|\mathbf{x}_j-\mathbf{x}_i\|}\left[(v_j-v_i)v_j-(v_j-v_i)v_i\right]=\frac{1}{2}\sum_{i=1}^{n}\sum_{j\in\chi_i}m(\Gamma_{ij})a_{ij}\|\mathbf{x}_j-\mathbf{x}_i\|\left(\frac{v_j-v_i}{\|\mathbf{x}_j-\mathbf{x}_i\|}\right)^2.$$

Since $\|\mathbf{x}_j - \mathbf{x}_i\| \geqslant \frac{1}{2}\mathrm{d}(\mathbf{x}_j, \mathbf{x}_i)$ for small enough h and $a_{ij} > \alpha_1$, we have

$$I_1 \geqslant \frac{\alpha_1}{2}|v|^2_{1,\mathscr{W}}. \tag{3.7}$$

On the other hand,

$$I_2 = \frac{1}{2}\sum_{i=1}^{n}\sum_{j\in\chi_i}\left[(\beta_{ij}+|\beta_{ij}|)v_i^2 + (\beta_{ij}-|\beta_{ij}|)v_jv_i\right] + \sum_{i=1}^{n} m(V_i)b_iv_i^2 = J_1 + J_2 + J_3,$$

where

$$J_1 = \frac{1}{2}\sum_{i=1}^{n}\left(\sum_{j\in\chi_i}\beta_{ij} + m(V_i)b_i\right)v_i^2, \qquad J_2 = \frac{1}{2}\sum_{i=1}^{n}\sum_{j\in\chi_i}|\beta_{ij}|(v_i - v_j)v_i,$$

and

$$J_3 = \frac{1}{2}\sum_{i=1}^{n}\left(\sum_{j\in\chi_i}\beta_{ij}v_iv_j + m(V_i)b_iv_i^2\right).$$

Through some calculations, we obtain

$$J_1 \geqslant \sum_{i=1}^{n}\frac{\alpha_2}{2}m(V_i)v_i^2 = \frac{\alpha_2}{2}\|v\|^2_{0,\mathscr{W}}, \qquad J_2 = \frac{1}{4}\sum_{i=1}^{n}\sum_{j\in\chi_i}|\beta_{ij}|(v_i - v_j)^2 \geqslant 0,$$

and

$$J_3 = \frac{1}{4}\sum_{i=1}^{n}\sum_{j\in\chi_i}(\beta_{ij}v_iv_j + \beta_{ji}v_iv_j) + \frac{1}{2}\sum_{i=1}^{n}b_iv_i^2 = \frac{1}{2}\sum_{i=1}^{n}b_iv_i^2 \geqslant 0$$

so that

$$I_2 > \frac{\alpha_2}{2}\|v\|^2_{0,\mathscr{W}}. \tag{3.8}$$

Combining (3.7) and (3.8), we finally obtain

$$(L^hv, v) \geqslant C\|v\|^2_{1,\mathscr{W}}$$

with $C = \min(\alpha_1/2, \alpha_2/2)$. □

Corollary 2. *The approximate solution defined by* (3.5) *satisfies the stability estimate*

$$\|u^h\|_{1,\mathscr{W}} \leqslant C\|f^h\|_{-1,\mathscr{W}},$$

where $f^h(\mathbf{x})$ *is a grid function on* $\mathbf{S}^2$ *such that* $f^h(\mathbf{x}) = f_i$ *if* $\mathbf{x} \in V_i$.

Proof. The result follows directly from Proposition 2. □

4. Error estimate

We will derive an error estimate using the framework of [9,10,16]. Without loss of generality, we set $a(\mathbf{x}) = 1$ in the following proof, i.e., $a_{ij} = 1$. For $\mathbf{x}_i$ and $\mathbf{x}_j$ that are neighbors, we also assume that $\frac{1}{2}\mathrm{d}(\mathbf{x}_i, \mathbf{x}_j) < \|\mathbf{x}_i - \mathbf{x}_j\| < \mathrm{d}(\mathbf{x}_i, \mathbf{x}_j)$ and $\frac{1}{2}m(\Gamma_{ij}) < \|\Gamma_{ij}\| < m(\Gamma_{ij})$, where $\|\Gamma_{ij}\|$ denotes the Euclidean distance

between the two end points of Γ_{ij}. Clearly, the latter two assumptions can be satisfied if h is sufficiently small. Denote by $\widetilde{\mathscr{E}}_{\mathbf{x}_k,\Gamma_{ij}}$ the spherical triangle determined by Γ_{ij} and $\mathbf{x}_k$, where $k = i$ or j, and set $\widetilde{\mathscr{E}}_{\Gamma_{ij}} = \widetilde{\mathscr{E}}_{\mathbf{x}_i,\Gamma_{ij}} \cup \widetilde{\mathscr{E}}_{\mathbf{x}_j,\Gamma_{ij}}$. Also, let

$$\mathscr{E}_{\mathbf{x}_k,\Gamma_{ij}} = \left\{ t\mathbf{x} + (1-t)\mathbf{x}_k \,|\, \mathbf{x} \in \Gamma_{ij}, t \in [0,1] \right\} \quad \text{for } k = i, j.$$

It is easy to see that $\widetilde{\mathscr{E}}_{\mathbf{x}_k,\Gamma_{ij}}$ is the normal projection of $\mathscr{E}_{\mathbf{x}_k,\Gamma_{ij}}$ on $\mathbf{S}^2$.

Suppose that Assumption 1 is satisfied and that $u \in H^2(\mathbf{S}^2)$ is the exact solution of (1.1). We then define, for $i = 1, \ldots, n$ and $j \in \chi_i$,

$$\begin{cases} \eta_{ij} = -\dfrac{1}{m(\Gamma_{ij})} \displaystyle\int_{\Gamma_{ij}} \nabla_s u(\mathbf{x}) \cdot \vec{\mathbf{n}}_{\mathbf{x},V_i} \, \mathrm{d}\gamma(\mathbf{x}) + \frac{u(\mathbf{x}_j) - u(\mathbf{x}_i)}{\|\mathbf{x}_j - \mathbf{x}_i\|}, \\ \mu_{ij} = \dfrac{1}{m(\Gamma_{ij})} \displaystyle\int_{\Gamma_{ij}} (\vec{\mathbf{v}}(\mathbf{x}) u(\mathbf{x})) \cdot \vec{\mathbf{n}}_{\mathbf{x},V_i} \, \mathrm{d}\gamma(\mathbf{x}) - \dfrac{1}{m(\Gamma_{ij})} (\beta_{ij}^{+} u(\mathbf{x}_i) + \beta_{ij}^{-} u(\mathbf{x}_j)), \\ \xi_i = \dfrac{1}{m(V_i)} \displaystyle\int_{V_i} b(x)(u(\mathbf{x}) - u(\mathbf{x}_k)) \, \mathrm{d}s(\mathbf{x}). \end{cases} \tag{4.1}$$

Before estimating the quantities defined in (4.1), let us first extend u, by projection, to a compact three-dimensional domain. Set $\Omega = \left\{ \mathbf{x} \,|\, 2r \geqslant \|\mathbf{x}\| \geqslant \frac{r}{2} \right\}$. It is easy to see that $\widetilde{\mathscr{E}}_{\mathbf{x}_i,\Gamma_{ij}} \subset \Omega$ and $\mathscr{E}_{\mathbf{x}_i,\Gamma_{ij}} \subset \Omega$ when h is small enough. Define

$$U(\mathbf{x}) = u\left(\frac{r}{\|\mathbf{x}\|} \mathbf{x} \right) \quad \text{for } \mathbf{x} \in \Omega. \tag{4.2}$$

Clearly, $U(\mathbf{x}) = u(\mathbf{x})$ if $\mathbf{x} \in \mathbf{S}^2$ and U does not depend on r if spherical coordinates are used, i.e., $\nabla U(\mathbf{x}) \cdot \vec{\mathbf{n}}_{\mathbf{S}^2,\mathbf{x}} = \nabla U(\mathbf{x}) \cdot \frac{\mathbf{x}}{\|\mathbf{x}\|} = 0$.

Lemma 1. *Let U be defined by* (4.2). *Then, for any $\mathbf{x}_i$ and $\mathbf{x}_j$ that are neighbors, we have the following results.*

1. *For any integer $q > 0$, there exists a constant $C_1 > 0$ such that*

$$\left(\int_{\mathscr{E}_{\mathbf{x}_k,\Gamma_{ij}}} |\nabla U(\mathbf{x})|^q \, \mathrm{d}s(\mathbf{x}) \right)^{1/q} \leqslant C_1 \|u\|_{W^{1,q}(\tilde{\mathscr{E}}_{\mathbf{x}_k,\Gamma_{ij}})} \quad \text{for } k = i, j,$$

   where $|\nabla U(\mathbf{x})|^2 = \sum_{i=1}^{3} |D_i U(\mathbf{x})|^2$.
2. *Let $H(U)(\mathbf{x})$ denote the Hessian matrix of U at the point $\mathbf{x}$. Then, there exists a constant $C_2 > 0$ such that*

$$\left(\int_{\mathscr{E}_{\mathbf{x}_k,\Gamma_{ij}}} |H(U)(\mathbf{x})|^2 \, \mathrm{d}s(\mathbf{x}) \right)^{1/2} \leqslant C_2 \|u\|_{H^2(\tilde{\mathscr{E}}_{\mathbf{x}_k,\Gamma_{ij}})} \quad \text{for } k = i, j,$$

   where $|H(U)(\mathbf{x})|^2 = \sum_{i,j=1}^{3} |D_i D_j U(\mathbf{x})|^2$.

Proof. For any $\mathbf{y} = (y_1, y_2, y_3) \in \mathbf{S}^2$, since $\nabla U(\mathbf{y}) \cdot \vec{\mathbf{n}}_{\mathbf{S}^2,\mathbf{y}} = 0$, we have

$$\nabla_s u(\mathbf{y}) = \nabla_s U(\mathbf{y}) = \nabla U(\mathbf{y}) - (\nabla U(\mathbf{y}) \cdot \vec{\mathbf{n}}_{\mathbf{S}^2,\mathbf{y}}) \vec{\mathbf{n}}_{\mathbf{S}^2,\mathbf{y}} = \nabla U(\mathbf{y}),$$

where $\vec{\mathbf{n}}_{\mathbf{S}^2,\mathbf{y}} = (y_1/r, y_2/r, y_3/r)$.

For any $\mathbf{x} = (x_1, x_2, x_3) \in \Omega$ with $\|\mathbf{x}\| < r$, let $\mathbf{y} = \frac{r}{\|\mathbf{x}\|} \mathbf{x} \in \mathbf{S}^2$, clearly, we have that, $\vec{\mathbf{n}}_{\mathbf{S}^2,\mathbf{y}} = (x_1/\|\mathbf{x}\|, x_2/\|\mathbf{x}\|, x_3/\|\mathbf{x}\|)$. Then, by the definition of $U(\mathbf{x})$ in (4.2), we have

$$\nabla U(\mathbf{x}) = \frac{r}{\|\mathbf{x}\|}\nabla U(\mathbf{y}) - \frac{r}{\|\mathbf{x}\|}\begin{pmatrix} \frac{x_1^2}{\|\mathbf{x}\|^2} & \frac{x_1x_2}{\|\mathbf{x}\|^2} & \frac{x_1x_3}{\|\mathbf{x}\|^2} \\ \frac{x_2x_1}{\|\mathbf{x}\|^2} & \frac{x_2^2}{\|\mathbf{x}\|^2} & \frac{x_2x_3}{\|\mathbf{x}\|^2} \\ \frac{x_3x_1}{\|\mathbf{x}\|^2} & \frac{x_3x_2}{\|\mathbf{x}\|^2} & \frac{x_3^2}{\|\mathbf{x}\|^2} \end{pmatrix}\nabla U(\mathbf{y})$$

$$= \frac{r}{\|\mathbf{x}\|}\left[\nabla U(\mathbf{y}) - \frac{1}{\|\mathbf{x}\|}\left(\nabla U(\mathbf{y})\cdot\vec{\mathbf{n}}_{\mathbf{S}^2,\mathbf{y}}\right)\begin{pmatrix} x_1 \\ x_2 \\ x_3 \end{pmatrix}\right]$$

$$= \frac{r}{\|\mathbf{x}\|}\nabla_s u(\mathbf{y}) = \frac{r}{\|\mathbf{x}\|}\nabla U(\mathbf{y}).$$

Since $r/\|\mathbf{x}\| \leqslant 2$, there exists a constant $\widetilde{C}_1 > 0$ depending only on $q > 0$ such that $|\nabla U(\mathbf{x})|^q \leqslant \widetilde{C}_1|\nabla U(\mathbf{y})|^q = \widetilde{C}_1|\nabla_s u(\mathbf{y})|^q$. On the other hand, it is obvious that $\mathbf{y} \in \tilde{\mathscr{E}}_{\mathbf{x}_i,\Gamma_{ij}}$ if $\mathbf{x} \in \mathscr{E}_{\mathbf{x}_i,\Gamma_{ij}}$ and $\mathrm{d}s(\mathbf{x}) \leqslant 2\,\mathrm{d}s(\mathbf{y})$ in this case so that, by integration and Holder inequality, we have

$$\left(\int_{\mathscr{E}_{\mathbf{x}_i,\Gamma_{ij}}} |\nabla U(\mathbf{x})|^q\,\mathrm{d}s(\mathbf{x})\right)^{1/q} \leqslant \widetilde{C}_1\left(\int_{\tilde{\mathscr{E}}_{\mathbf{x}_i,\Gamma_{ij}}} |\nabla_s u(\mathbf{y})|^q\,\mathrm{d}s(\mathbf{y})\right)^{1/q} \leqslant C_1\|u\|_{W^{1,q}(\tilde{\mathscr{E}}_{\mathbf{x}_i,\Gamma_{ij}})}$$

for some constant C_1 only depending on q. Similarly, we have

$$\left(\int_{\mathscr{E}_{\mathbf{x}_j,\Gamma_{ij}}} |\nabla U(\mathbf{x})|^q\,\mathrm{d}s(\mathbf{x})\right)^{1/q} \leqslant C_1\|u\|_{W^{1,q}(\tilde{\mathscr{E}}_{\mathbf{x}_j,\Gamma_{ij}})}.$$

By a similar but more tedious calculation, we can find that, for any $\mathbf{y} \in \mathbf{S}^2$,

$$\nabla(D_iU)(\mathbf{y}) = \nabla_s(\nabla_{s,i}u)(\mathbf{y}) - \frac{1}{r}(\nabla_{s,i}u(\mathbf{y}))\vec{\mathbf{n}}_{\mathbf{S}^2,\mathbf{y}} \quad \text{for } i = 1,2,3$$

then we know that, for some constant $C_3 > 0$,

$$\sum_{i,j=1}^{3} |D_iD_jU(\mathbf{y})|^2 \leqslant C_3 \sum_{0\leqslant|\alpha|\leqslant 2} |\nabla_s^\alpha u(\mathbf{y})|^2.$$

Also for any $\mathbf{x} \in \Omega$, let $\mathbf{y} = \frac{r}{\|\mathbf{x}\|}\mathbf{x}$, we have

$$D_iD_jU(\mathbf{x}) = D_i\left(\frac{r}{\|\mathbf{x}\|}D_jU(\mathbf{y})\right) = \frac{r^2}{\|\mathbf{x}\|^2}D_iD_jU(\mathbf{y}).$$

So there exists a constant $\widetilde{C}_2 > 0$ such that

$$|H(U)(\mathbf{x})|^2 \leqslant \widetilde{C}_2 \sum_{0\leqslant|\alpha|\leqslant 2} |\nabla_s^\alpha U(\mathbf{y})|^2.$$

Then, by integration, we have that, for some constant $C_2 > 0$,

$$\left(\int_{\mathscr{E}_{\mathbf{x}_k,\Gamma_{ij}}} |H(U)(\mathbf{x})|^2\,\mathrm{d}s(\mathbf{x})\right)^{1/2} \leqslant C_2\|u\|_{H^2(\tilde{\mathscr{E}}_{\mathbf{x}_k,\Gamma_{ij}})} \quad \text{for } k = i,j. \qquad \square$$

Proposition 3. *Suppose that Assumption* 1 *is satisfied. Let* σ *be defined by* (2.2) *and let* η_{ij}, μ_{ij}, *and* ξ_i *be defined by* (4.1). *Let u be the unique variational solution of* (1.1) *which belongs to* $H^2(\mathbf{S}^2)$ *and satisfies equations* (1.3). *Then, there exist constants* $C_3 > 0$ *and* $C_4 > 0$ *depending on* $\vec{\mathbf{v}}$ *and q and* $C_5 > 0$ *only depending on b and q such that, for any* $\mathbf{x}_i$ *and* $\mathbf{x}_j$ *that are neighbors,*

$$\eta_{ij} \leqslant \frac{C_3 h}{\sigma^{3/2}\sqrt{m(\Gamma_{ij})\,\mathrm{d}(\mathbf{x}_i,\mathbf{x}_j)}}\,\|u\|_{H^2(\widetilde{\mathscr{E}}_{\Gamma_{ij}})}, \tag{4.3}$$

$$\mu_{ij} \leqslant \frac{C_4 h}{(m(\Gamma_{ij})\,\mathrm{d}(\mathbf{x}_i,\mathbf{x}_j))^{1/q}}\,\|u\|_{W^{1,q}(\widetilde{\mathscr{E}}_{\mathbf{x}_i,\Gamma_{ij}})}, \tag{4.4}$$

and

$$\xi_i \leqslant \frac{C_5 h}{(m(V_i))^{1/q}}\,\|u\|_{W^{1,q}(V_i)} \tag{4.5}$$

for any integer $q > 2$.

Proof. For this proof, we use some techniques similar to those used in [10]. First, due to Sobolev imbedding theorems in a compact, two-dimensional Riemannian manifold [11], if $u \in H^2(\mathbf{S}^2)$, then $u \in W^{1,q}(\mathbf{S}^2)$ for all $q > 2$ so that (4.4) and (4.5) are well-defined. Since $u \in H^2(\mathbf{S}^2)$, the restriction of u to $\widetilde{\mathscr{E}}_{\Gamma_{ij}}$ also belongs to $H^2(\widetilde{\mathscr{E}}_{\Gamma_{ij}})$. We know that $C^2(\overline{\widetilde{\mathscr{E}}_{\Gamma_{ij}}})$ is dense in $H^2(\widetilde{\mathscr{E}}_{\Gamma_{ij}})$, so we only need to prove (4.3)–(4.5) for $u \in C^2(\overline{\widetilde{\mathscr{E}}_{\Gamma_{ij}}})$ and then use a density argument; see [17].

Let us assume that $u \in C^2(\overline{\widetilde{\mathscr{E}}_{\Gamma_{ij}}})$. Define $\Omega_{ij} = \left\{\mathbf{x} \in \Omega \,\middle|\, r\frac{\mathbf{x}}{\|\mathbf{x}\|} \in \widetilde{\mathscr{E}}_{\Gamma_{ij}}\right\}$. Then, it is easy to see that $U \in C^2(\overline{\Omega_{ij}})$. By Taylor's theorem, we have for, any $\mathbf{x} \in \Gamma_{ij}$,

$$\begin{aligned} u(\mathbf{x}_i) - u(\mathbf{x}) &= U(\mathbf{x}_i) - U(\mathbf{x}) \\ &= \nabla U(\mathbf{x}) \cdot (\mathbf{x}_i - \mathbf{x}) + \int_0^1 H(U)(t\mathbf{x} + (1-t)\mathbf{x}_i)(\mathbf{x}_i - \mathbf{x}) \cdot (\mathbf{x}_i - \mathbf{x}) t\,\mathrm{d}t \end{aligned} \tag{4.6}$$

and similarly

$$u(\mathbf{x}_j) - u(\mathbf{x}) = \nabla U(\mathbf{x}) \cdot (\mathbf{x}_j - \mathbf{x}) + \int_0^1 H(U)(t\mathbf{x} + (1-t)\mathbf{x}_j)(\mathbf{x}_j - \mathbf{x}) \cdot (\mathbf{x}_j - \mathbf{x}) t\,\mathrm{d}t. \tag{4.7}$$

Note that we have $\mathbf{x}_j - \mathbf{x}_i = \|\mathbf{x}_j - \mathbf{x}_i\|\vec{\mathbf{n}}_{\mathbf{x},V_i}$ from (2.1) and

$$\nabla_s u(\mathbf{x}) \cdot \vec{\mathbf{n}}_{\mathbf{x},V_i} = \nabla u(\mathbf{x}) \cdot \vec{\mathbf{n}}_{\mathbf{x},V_i} - (\nabla u(\mathbf{x}) \cdot \vec{\mathbf{n}}_{\mathbf{S}^2,\mathbf{x}})(\vec{\mathbf{n}}_{\mathbf{S}^2,\mathbf{x}} \cdot \vec{\mathbf{n}}_{\mathbf{x},V_i}) = \nabla u(\mathbf{x}) \cdot \vec{\mathbf{n}}_{\mathbf{x},V_i} = \nabla U(\mathbf{x}) \cdot \vec{\mathbf{n}}_{\mathbf{x},V_i}.$$

Subtracting (4.6) from (4.7) and integrating over Γ_{ij}, we obtain, for some constant $\widetilde{C}_3 > 0$,

$$\left| m(\Gamma_{ij})(u(\mathbf{x}_j) - u(\mathbf{x}_i)) - \|\mathbf{x}_j - \mathbf{x}_i\| \int_{\Gamma_{ij}} \nabla_s u(\mathbf{x}) \cdot \vec{\mathbf{n}}_{\mathbf{x},V_i}\,\mathrm{d}\gamma(\mathbf{x}) \right| \leqslant \widetilde{C}_3(P_i + P_j)$$

with

$$P_k = \int_{\Gamma_{ij}} \int_0^1 |H(U)(t\mathbf{x} + (1-t)\mathbf{x}_k)|\|\mathbf{x}_k - \mathbf{x}\|^2 t\,\mathrm{d}t\,\mathrm{d}\gamma(\mathbf{x}) \quad \text{for } k = i, j$$

so that

$$|\eta_{ij}| \leqslant \frac{\widetilde{C}_3}{m(\Gamma_{ij})\|x_j - x_i\|}(P_i + P_j) \leqslant \frac{2\widetilde{C}_3}{m(\Gamma_{ij})\,\mathrm{d}(x_j, x_i)}(P_i + P_j). \tag{4.8}$$

To estimate P_i, set $\mathbf{y} = t\mathbf{x} + (1-t)\mathbf{x}_i$. We know that $|\mathbf{x}_i - \mathbf{x}| \leqslant h_i$ and, if h_i is small enough,

$$m(\mathscr{E}_{\mathbf{x}_i,\Gamma_{ij}}) \leqslant \frac{h_i m(\Gamma_{ij})}{2} \leqslant \frac{\mathrm{d}(\mathbf{x}_i,\mathbf{x}_j) m(\Gamma_{ij})}{4\sigma}$$

and

$$\mathrm{d}s(\mathbf{y}) \geqslant \tfrac{1}{2} t \|\mathbf{x}_i - \mathbf{x}_j\| \,\mathrm{d}t\,\mathrm{d}\gamma(\mathbf{x}) \geqslant \tfrac{1}{4} t\,\mathrm{d}(\mathbf{x}_i,\mathbf{x}_j)\,\mathrm{d}t\,\mathrm{d}\gamma(\mathbf{x}).$$

Then, we have by the Cauchy–Schwarz inequality that

$$\begin{aligned} P_i &\leqslant \frac{4h_i^2}{\mathrm{d}(\mathbf{x}_i,\mathbf{x}_j)} \int_{\mathscr{E}_{\mathbf{x}_i,\Gamma_{ij}}} |H(U)(\mathbf{y})|\,\mathrm{d}s(\mathbf{y}) \\ &\leqslant \frac{4h_i^2}{\mathrm{d}(\mathbf{x}_i,\mathbf{x}_j)} \left(\int_{\mathscr{E}_{\mathbf{x}_i,\Gamma_{ij}}} |H(U)(\mathbf{y})|^2\,\mathrm{d}s(\mathbf{y}) \right)^{1/2} \left(\int_{\mathscr{E}_{\mathbf{x}_i,\Gamma_{ij}}} \mathrm{d}s(\mathbf{y}) \right)^{1/2} \\ &\leqslant \frac{2h_i^2\sqrt{m(\Gamma_{ij})}}{\sqrt{\sigma\,\mathrm{d}(\mathbf{x}_i,\mathbf{x}_j)}} \left(\int_{\mathscr{E}_{\mathbf{x}_i,\Gamma_{ij}}} |H(U)(\mathbf{y})|^2\,\mathrm{d}s(\mathbf{y}) \right)^{1/2}. \end{aligned} \tag{4.9}$$

Similarly, we obtain

$$P_j \leqslant \frac{2h_j^2\sqrt{m(\Gamma_{ij})}}{\sqrt{\sigma\,\mathrm{d}(\mathbf{x}_i,\mathbf{x}_j)}} \left(\int_{\mathscr{E}_{\mathbf{x}_j,\Gamma_{ij}}} |H(U)(\mathbf{y})|^2\,\mathrm{d}s(\mathbf{y}) \right)^{1/2}. \tag{4.10}$$

Combining (4.8)–(4.10) we obtain, by Lemma 1, that

$$\begin{aligned} |\eta_{ij}| &\leqslant \frac{2\widetilde{C}_3 h_i}{\sigma^{3/2}\sqrt{m(\Gamma_{ij})\,\mathrm{d}(\mathbf{x}_i,\mathbf{x}_j)}} \|u\|_{H^2(\tilde{\mathscr{E}}_{\mathbf{x}_i,\Gamma_{ij}})} + \frac{2\widetilde{C}_3 h_j}{\sigma^{3/2}\sqrt{m(\Gamma_{ij})\,\mathrm{d}(\mathbf{x}_i,\mathbf{x}_j)}} \|u\|_{H^2(\tilde{\mathscr{E}}_{\mathbf{x}_i,\Gamma_{ij}})} \\ &\leqslant \frac{C_3 h}{\sigma^{3/2}\sqrt{m(\Gamma_{ij})\,\mathrm{d}(\mathbf{x}_i,\mathbf{x}_j)}} \|u\|_{H^2(\tilde{\mathscr{E}}_{\Gamma_{ij}})}. \end{aligned}$$

Now we invoke the density argument. Let $u \in H^2(\widetilde{\mathscr{E}}_{\Gamma_{ij}})$ and $\{u_n \in C^2(\overline{\widetilde{\mathscr{E}}_{\Gamma_{ij}}})\}_{n=1}^{\infty}$ be a sequence which converges to u in the $H^2(\widetilde{\mathscr{E}}_{\Gamma_{ij}})$ norm [11,17]. Then, we have, as above, that

$$\left| -\frac{1}{m(\Gamma_{ij})} \int_{\Gamma_{ij}} \nabla_s u_n(\mathbf{x}) \cdot \vec{\mathbf{n}}_{\mathbf{x},V_i}\,\mathrm{d}\gamma(\mathbf{x}) + \frac{u_n(\mathbf{x}_j) - u_n(\mathbf{x}_i)}{\|\mathbf{x}_j - \mathbf{x}_i\|} \right| \leqslant \frac{C_3 h}{\sigma^{3/2}\sqrt{m(\Gamma_{ij})\,\mathrm{d}(\mathbf{x}_i,\mathbf{x}_j)}} \|u_n\|_{H^2(\tilde{\mathscr{E}}_{\Gamma_{ij}})}.$$

Again, Sobolev imbedding theorems in the compact manifold $\mathbf{S}^2$ guarantee that u_n converges to u uniformly in $H^2(\widetilde{\mathscr{E}}_{\Gamma_{ij}})$ and $\nabla_s u_n(\mathbf{x}) \cdot \vec{\mathbf{n}}_{\mathbf{x},V_i}$ converges to $\nabla_s u(\mathbf{x}) \cdot \vec{\mathbf{n}}_{\mathbf{x},V_i}$ in $L^1(\widetilde{\mathscr{E}}_{\Gamma_{ij}})$. Passing to the limit yields (4.3) for $u \in H^2(\widetilde{\mathscr{E}}_{\Gamma_{ij}})$.

Next, let us turn to the estimation of μ_{ij}. Assume, without loss of generality, that $\beta_{ij} \geqslant 0$. Then,

$$\mu_{ij} = \frac{1}{m(\Gamma_{ij})} \int_{\Gamma_{ij}} (\vec{\mathbf{v}}(\mathbf{x}) \cdot \vec{\mathbf{n}}_{\mathbf{x},V_i})(u(\mathbf{x}) - u(\mathbf{x}_i))\,\mathrm{d}\gamma(\mathbf{x}).$$

Applying Taylor's theorem using $u \in C^1(\widetilde{\mathscr{E}}_{\Gamma_{ij}})$, we have

$$\begin{aligned} |\mu_{ij}| &\leqslant \frac{\sup_{\mathbf{x}\in\overline{\mathbf{S}}^2} |\vec{\mathbf{v}}(\mathbf{x})|}{m(\Gamma_{ij})} \int_{\Gamma_{ij}} \int_0^1 |\nabla U(t\mathbf{x} + (1-t)\mathbf{x}_i)| \|\mathbf{x}_i - \mathbf{x}\|\,\mathrm{d}t\,\mathrm{d}\gamma(\mathbf{x}) \\ &\leqslant \frac{h_i \sup_{\mathbf{x}\in\overline{\mathbf{S}}^2} |\vec{\mathbf{v}}(\mathbf{x})|}{m(\Gamma_{ij})} \int_{\Gamma_{ij}} \int_0^1 |\nabla U(t\mathbf{x} + (1-t)\mathbf{x}_i)|\,\mathrm{d}t\,\mathrm{d}\gamma(\mathbf{x}), \end{aligned}$$

where $|\vec{\mathbf{v}}(\mathbf{x})| = \sum_{i=1}^{3} |v_i(\mathbf{x})|$. For $q > 2$, choose p such that $\frac{1}{q} + \frac{1}{p} = 1$. By Holder's inequality, we have

$$\int_{\Gamma_{ij}} \int_0^1 |\nabla U(t\mathbf{x} + (1-t)\mathbf{x}_i)| \, \mathrm{d}t \, \mathrm{d}\gamma(\mathbf{x})$$
$$\leqslant \left(\int_{\Gamma_{ij}} \int_0^1 |\nabla U(t\mathbf{x} + (1-t)\mathbf{x}_i)|^q t \, \mathrm{d}t \, \mathrm{d}\gamma(\mathbf{x}) \right)^{1/q} \cdot \left(\int_{\Gamma_{ij}} \int_0^1 \frac{1}{t^{p/q}} \, \mathrm{d}t \, \mathrm{d}\gamma(\mathbf{x}) \right)^{1/p}.$$

Since $q > 2$, we know $p/q < 1$. By a similar change of variables as was used before and Lemma 1, we have

$$|\mu_{ij}| \leqslant \frac{4^{1/q} h_i \sup_{\mathbf{x} \in \bar{\mathbf{S}}^2} |\vec{\mathbf{v}}(\mathbf{x})|}{m(\Gamma_{ij})(\mathrm{d}(\mathbf{x}_i, \mathbf{x}_j))^{1/q}} \left(\int_{\mathscr{E}_{\mathbf{x}_i, \Gamma_{ij}}} |\nabla U(\mathbf{y})|^q \, \mathrm{d}s(\mathbf{y}) \right)^{1/q} \left(\int_{\Gamma_{ij}} \int_0^1 \frac{1}{t^{p/q}} \, \mathrm{d}t \, \mathrm{d}\gamma(\mathbf{x}) \right)^{1/p}$$
$$\leqslant \frac{C_7 h_i \big(m(\Gamma_{ij})\big)^{1/p}}{m(\Gamma_{ij})(\mathrm{d}(\mathbf{x}_i, \mathbf{x}_j))^{1/q}} \|u\|_{W^{1,q}(\mathscr{E}_{\mathbf{x}_i, \bar{\Gamma}_{ij}})} \left(\int_0^1 \frac{1}{t^{p/q}} \, \mathrm{d}t \right)^{1/p}$$
$$\leqslant \frac{C_4 h}{(m(\Gamma_{ij}) \, \mathrm{d}(\mathbf{x}_i, \mathbf{x}_j))^{1/q}} \|u\|_{W^{1,q}(\mathscr{E}_{\mathbf{x}_i, \bar{\Gamma}_{ij}})}.$$

Then, we obtain (4.4) for $u \in H^2(\widetilde{\mathscr{E}}_{\Gamma_{ij}})$ by again invoking a density argument.

Finally, let us estimate ξ_i. Assume that $u \in C^2(V_i)$. Using Taylor's theorem, we have

$$|\xi_i| \leqslant \frac{\|b\|_{L^\infty(\mathbf{S}^2)} h_i}{m(V_i)} \int_{V_i} \int_0^1 |\nabla U(t\mathbf{x} + (1-t)\mathbf{x}_i)| \, \mathrm{d}t \, \mathrm{d}s(\mathbf{x}).$$

Changing variables by $\mathbf{y} = t\mathbf{x} + (1-t)\mathbf{x}_i$ and setting $V_i^t = \{\mathbf{y} = t\mathbf{x} + (1-t)\mathbf{x}_i \,|\, \mathbf{x} \in V_i\}$, we have that $\mathrm{d}s(\mathbf{x}) \leqslant 2 \, \mathrm{d}s(\mathbf{y})/t^2$ since $V_i^t - \partial V_i^t$ falls inside the $\mathbf{S}^2$. Then,

$$|\xi_i| \leqslant \frac{2\|b\|_{L^\infty(\mathbf{S}^2)} h_i}{m(V_i)} \int_0^1 \int_{V_i^t} \frac{|\nabla U(\mathbf{y})|}{t^2} \, \mathrm{d}s(\mathbf{y}) \, \mathrm{d}t.$$

It is not difficult to see that $m(V_i^t) \leqslant t^2 m(V_i)$. By Holder's inequality and a similar proof procedure as that for Lemma 1, we obtain

$$|\xi_i| \leqslant \frac{2\|b\|_{L^\infty(\mathbf{S}^2)} h_i}{m(V_i)} \int_0^1 \left(\int_{V_i^t} |\nabla U(\mathbf{y})|^q \, \mathrm{d}s(\mathbf{y}) \right)^{1/q} (m(V_i^t))^{1/p} \frac{1}{t^2} \, \mathrm{d}t$$
$$\leqslant \frac{2\|b\|_{L^\infty(\mathbf{S}^2)} h_i}{m(V_i)} \|u\|_{W^{1,q}(V_i)} (m(V_i))^{1/p} \int_0^1 \frac{1}{t^{2/q}} \, \mathrm{d}t$$
$$\leqslant \frac{C_5 h}{(m(V_i))^{1/q}} \|u\|_{W^{1,q}(V_i)}.$$

Then, we obtain (4.5) for $u \in H^2(V_i)$ by again invoking a density argument. □

Now we can prove the convergence of the finite volume discretization scheme. Define the *grid error function* e^h by

$$e^h(\mathbf{x}) = e_i^h = u(\mathbf{x}_i) - u_i^h \quad \text{if } \mathbf{x} \in V_i. \tag{4.11}$$

We then have the following error estimate.

Theorem 1. *Suppose that Assumption* 1 *is satisfied. Let* $\mathscr{F}_{ij}$, $\mathscr{V}_{ij}$, *and* b_i *be defined by* (3.1)–(3.3) *and* σ *be defined by* (2.2). *Assume that the unique variational solution* u *of* (1.1) *belongs to* $H^2(\mathbf{S}^2)$. *Let* u^h *denote the solution of* (3.5) *and let* e^h *be defined by* (4.11). *Then, there exists a constant* $C > 0$ *only depending on* $\vec{\mathbf{v}}$, b, *and* σ *such that*

$$\|e^h\|_{1,\mathscr{W}} \leqslant Ch\|u\|_{H^2(\mathbf{S}^2)}. \tag{4.12}$$

Proof. By the definition of the discrete inner product, we have

$$(L^h e^h, e^h) = (L^h(u-u^h), e^h) = \sum_{i=1}^{n}\left(\sum_{j\in\chi_i} m(\Gamma_{ij})(\eta_{ij}e_i^h + \mu_{ij}e_i^h) + m(V_i)\xi_i e_i^h\right).$$

Define

$$\overline{\mathscr{F}}_{ij} = -\int_{\Gamma_{ij}} \nabla_s u(\mathbf{x})\cdot\vec{\mathbf{n}}_{\mathbf{x},V_i}\,\mathrm{d}\gamma(\mathbf{x}).$$

First, we have that

$$\begin{aligned}
\sum_{i=1}^{n}\sum_{j\in\chi_i} m(\Gamma_{ij})\eta_{ij}e_i^h &= \sum_{i=1}^{n}\sum_{j\in\chi_i}\left(\overline{\mathscr{F}}_{ij} + m(\Gamma_{ij})\frac{u(\mathbf{x}_j)-u(\mathbf{x}_i)}{\|\mathbf{x}_j-\mathbf{x}_i\|}\right)e_i^h \\
&= \frac{1}{2}\sum_{i=1}^{n}\sum_{j\in\chi_i}\left[\left(\overline{\mathscr{F}}_{ij} + m(\Gamma_{ij})\frac{u(\mathbf{x}_j)-u(\mathbf{x}_i)}{\|\mathbf{x}_j-\mathbf{x}_i\|}\right)e_i^h + \left(\overline{\mathscr{F}}_{ij} + m(\Gamma_{ij})\frac{u(\mathbf{x}_i)-u(\mathbf{x}_j)}{\|\mathbf{x}_j-\mathbf{x}_i\|}\right)e_j^h\right] \\
&= -\frac{1}{2}\sum_{i=1}^{n}\sum_{j\in\chi_i}\left(\overline{\mathscr{F}}_{ij} + m(\Gamma_{ij})\frac{u(\mathbf{x}_j)-u(\mathbf{x}_i)}{\|\mathbf{x}_j-\mathbf{x}_i\|}\right)(e_j^h - e_i^h) \\
&= -\frac{1}{2}\sum_{i=1}^{n}\sum_{j\in\chi_i}\|\mathbf{x}_i-\mathbf{x}_j\| m(\Gamma_{ij})\eta_{ij}\frac{e_j^h - e_i^h}{\|\mathbf{x}_i-\mathbf{x}_j\|}
\end{aligned}$$

so that, by the Cauchy–Schwartz inequality, we have that

$$\begin{aligned}
\left|\sum_{i=1}^{n}\sum_{j\in\chi_i} m(\Gamma_{ij})\eta_{ij}e_i^h\right| &\leqslant \frac{1}{2}\sum_{i=1}^{n}\sum_{j\in\chi_i}\mathrm{d}(\mathbf{x}_i,\mathbf{x}_j)m(\Gamma_{ij})\eta_{ij}\frac{|e_j^h - e_i^h|}{\|\mathbf{x}_i-\mathbf{x}_j\|} \\
&\leqslant \frac{\sqrt{2}}{2}\left(\sum_{i=1}^{n}\sum_{j\in\chi_i} m(\Gamma_{ij})\,\mathrm{d}(\mathbf{x}_i,\mathbf{x}_j)\eta_{ij}^2\right)^{1/2}\cdot\left(\sum_{i=1}^{n}\sum_{j\in\chi_i}\frac{1}{2}m(\Gamma_{ij})\,\mathrm{d}(\mathbf{x}_i,\mathbf{x}_j)\left(\frac{e_j^h - e_i^h}{\|\mathbf{x}_i-\mathbf{x}_j\|}\right)^2\right)^{1/2} \\
&\leqslant \frac{\sqrt{2}}{2}\left(\sum_{i=1}^{n}\sum_{j\in\chi_i} m(\Gamma_{ij})\,\mathrm{d}(\mathbf{x}_i,\mathbf{x}_j)\eta_{ij}^2\right)^{1/2}|e^h|_{1,\mathscr{W}}.
\end{aligned}$$

By Proposition 3, we obtain

$$\left|\sum_{i=1}^{n}\sum_{j\in\chi_i} m(\Gamma_{ij})\eta_{ij}e_i^h\right| \leqslant \frac{C_1 h}{\sigma^{3/2}}|e^h|_{1,\mathscr{W}}\left(\sum_{i=1}^{n}\sum_{j\in\chi_i}\|u\|^2_{H^2(\breve{\mathscr{E}}_{\Gamma_{ij}})}\right)^{1/2} \leqslant \frac{C_2 h}{\sigma^{3/2}}\|u\|_{H^2(\mathbf{S}^2)}|e^h|_{1,\mathscr{W}}. \tag{4.13}$$

Likewise, by Proposition 3,

$$\left|\sum_{i=1}^{n}\sum_{j\in\chi_i} m(\Gamma_{ij})\mu_{ij}e_i^h\right| \leqslant \frac{1}{2}\sum_{i=1}^{n}\sum_{j\in\chi_i}\|\mathbf{x}_i-\mathbf{x}_j\|m(\Gamma_{ij})\mu_{ij}\frac{|e_j^h-e_i^h|}{\|\mathbf{x}_i-\mathbf{x}_j\|}$$
$$\leqslant \frac{\sqrt{2}}{2}\left(\sum_{i=1}^{n}\sum_{j\in\chi_i} m(\Gamma_{ij})\,\mathrm{d}(\mathbf{x}_i,\mathbf{x}_j)\mu_{ij}^2\right)^{1/2}|e^h|_{1,\mathscr{W}}$$
$$\leqslant C_3 h|e^h|_{1,\mathscr{W}}\left(\sum_{i=1}^{n}\sum_{j\in\chi_i}\frac{\|u\|^2_{W^{1,q}(\tilde{\mathscr{E}}_{\mathbf{x}_i,\Gamma_{ij}})}}{\left(m(\Gamma_{ij})\,\mathrm{d}(\mathbf{x}_i,\mathbf{x}_j)\right)^{2/q-1}}\right)^{1/2}.$$

When h is sufficiently small, we have

$$m(\widetilde{\mathscr{E}}_{\mathbf{x}_i,\Gamma_{ij}}) \geqslant \tfrac{1}{4}\|\mathbf{x}_i-\mathbf{x}_j\|\cdot\|\Gamma_{ij}\| \geqslant \tfrac{1}{16}\mathrm{d}(\mathbf{x}_i,\mathbf{x}_j)m(\Gamma_{ij}).$$

By Holder's inequality and by letting $q=3$, we have

$$\left|\sum_{i=1}^{n}\sum_{j\in\chi_i} m(\Gamma_{ij})\mu_{ij}e_i^h\right| \leqslant C_4 h|e^h|_{1,\mathscr{W}}\left(\sum_{i=1}^{n}\sum_{j\in\chi_i}\left(m(\widetilde{\mathscr{E}}_{\mathbf{x}_i,\Gamma_{ij}})\right)^{1-2/q}\|u\|^2_{W^{1,q}(\tilde{\mathscr{E}}_{\mathbf{x}_i,\Gamma_{ij}})}\right)^{1/2}$$
$$\leqslant C_5 h|e^h|_{1,\mathscr{W}}\left(\left(m(\mathbf{S}^2)\right)^{1-2/q}\|u\|^2_{W^{1,q}(\mathbf{S}^2)}\right)^{1/2}$$
$$\leqslant C_6 h\|u\|_{W^{1,3}(\mathbf{S}^2)}|e^h|_{1,\mathscr{W}}. \tag{4.14}$$

Similar to the estimation of (4.14), we have that

$$\left|\sum_{i=1}^{n} m(V_i)\xi_i e_i^h\right| \leqslant \left(\sum_{i=1}^{n} m(V_i)\xi_i^2\right)^{1/2}\left(\sum_{i=1}^{n} m(V_i)(e_i^h)^2\right)^{1/2}$$
$$\leqslant C_7 h|e^h|_{0,\mathscr{W}}\left(\sum_{i=1}^{n}\left(m(V_i)\right)^{1-2/q}\|u\|^2_{W^{1,q}(V_i)}\right)^{1/2}$$
$$\leqslant C_7 h\left(\left(m(\mathbf{S}^2)\right)^{1-2/q}\|u\|^2_{W^{1,q}(\mathbf{S}^2)}\right)^{1/2}|e^h|_{0,\mathscr{W}} \leqslant C_8 h\|u\|_{W^{1,3}(\mathbf{S}^2)}|e^h|_{0,\mathscr{W}}. \tag{4.15}$$

Combining (4.13)–(4.15), by Proposition 2, we finally obtain

$$\|e^h\|_{1,\mathscr{W}} \leqslant C_9 h\left(C_2\sigma^{-3/2}\|u\|_{H^2(\mathbf{S}^2)} + C_6\|u\|_{W^{1,3}(\mathbf{S}^2)} + C_8\|u\|_{W^{1,3}(\mathbf{S}^2)}\right) \leqslant Ch\|u\|_{H^2(\mathbf{S}^2)}, \tag{4.16}$$

where C is a constant depending on $\vec{\mathbf{v}}$, b, and σ. □

Remark 2. If $u\in C^2(\mathbf{S}^2)$, the estimates (4.3)–(4.5), and (4.12) can be obtained straightforwardly by Taylor's expansion.

5. Optimal Voronoi meshes on the sphere

The error estimate (4.12) holds for any Voronoi tessellation of the sphere. However, the actual error, either asymptotically as the grid size tends to zero or for a fixed grid size, can differ dramatically for different particular Voronoi tessellations. Even the constant in the error estimate depends on grid parameters; most notably, it is proportional to $\sigma^{-3/2}$ (see (4.16)) so that for small values of σ the constant is relatively large. It is observed experimentally that the error itself exhibits similar dependence on σ. Therefore, we are

left with the problem of how to choose a "good" Voronoi mesh for the finite volume scheme, e.g., in general, how to choose the set of points $\{\mathbf{x}_i\}_{i=1}^m$ so that σ is "large."

In this section and the next, we examine special Voronoi meshes on the sphere which were introduced in [6] and which are referred to as *constrained centroidal Voronoi tessellations* (CCVTs). This class of meshes have many desirable properties, some of which are discussed in this section and in Section 6. After defining the CCVT class of meshes, we discuss, in this section and the next, an algorithm for their construction and we then use them to obtain finite volume approximations of solutions of the model problem (1.1).

5.1. Definition of CCVTs

Given a density function $\rho(\mathbf{x})$ defined on $\mathbf{S}^2$, for any region $V \subset \mathbf{S}^2$, we call $\mathbf{x}^c$ the *constrained mass centroid of V on $\mathbf{S}^2$* if $\mathbf{x}^c$ is a solution of the following problem:

$$\min_{\mathbf{x}\in V} F(\mathbf{x}), \quad \text{where} \quad F(\mathbf{x}) = \int_V \rho(\mathbf{y})\|\mathbf{y}-\mathbf{x}\|^2 \,\mathrm{d}s(\mathbf{y}). \tag{5.1}$$

The existence of solutions of (5.1) can be easily obtained using the continuity and compactness of F; however, solutions may not be unique. In general, given a Voronoi tessellation $\mathscr{W} = \{\mathbf{x}_i, V_i\}_{i=1}^n$ of $\mathbf{S}^2$, the generators $\{\mathbf{x}_i\}_{i=1}^n$ do not coincide with $\{\mathbf{x}_i^c\}_{i=1}^n$, where $\mathbf{x}_i^c$, $i = 1,\ldots,n$, denotes the constrained mass centroid of V_i. We refer to a Voronoi tessellation $\mathbf{S}^2$ as a *constrained centroidal Voronoi tessellation* (CCVT) if and only if the points $\{\mathbf{x}_i\}_{i=1}^m$ which serve as the generators of the associated Voronoi tessellation $\{V_i\}_{i=1}^k$ are also the constrained mass centroids of those regions, i.e., if and only if we have that

$$\mathbf{x}_i = \mathbf{x}_i^c \quad \text{for } i = 1,\ldots,n.$$

For more detailed studies on constrained centroidal Voronoi tessellations and general centroidal Voronoi tessellations, we refer to [5,6].

Given any set of points $\{\tilde{\mathbf{x}}_i\}_{i=1}^n$ on $\mathbf{S}^2$ and any tessellation $\{\widetilde{V}_i\}_{i=1}^n$ of $\mathbf{S}^2$, we define the corresponding *energy* by

$$\mathscr{K}\left(\{\tilde{\mathbf{x}}_i, \widetilde{V}_i\}_{i=1}^n\right) = \sum_{i=1}^n \int_{\widetilde{V}_i} \rho(\mathbf{y})\|\mathbf{y}-\tilde{\mathbf{x}}_i\|^2 \,\mathrm{d}s(\mathbf{y}).$$

A priori, there is no assumed condition between the points set $\{\tilde{\mathbf{x}}_i\}_{i=1}^n$ and the tessellation $\{\widetilde{V}_i\}_{i=1}^n$. However, it can be shown that $\mathscr{K}(\cdot)$ is minimized only if $\{\tilde{\mathbf{x}}_i, \widetilde{V}_i\}_{i=1}^n$ are a constrained centroidal Voronoi tessellation. Although the *energy* $\mathscr{K}$ may not be directly identified with the energy of some physical system, it is often naturally associated with quantities such as error distorsion, variance and cost in many practical applications [5]. The energy is equally distributed on each $\widetilde{V}_i$ in an asymptotic way. As a consequence, constrained centroidal Voronoi meshes on the sphere have many good geometric properties, including the following.

- For a constant density function, the generators $\{\mathbf{x}_i\}_{i=1}^m$ are uniformly distributed in some sense; the V_i's are all almost of the same size and most of them are similar convex spherical hexagons; the mesh size h is approximately proportional to $1/\sqrt{n}$.
- For a non-constant density function, the generators $\{\mathbf{x}_i\}_{i=1}^m$ are still locally uniformly distributed and it is conjectured that, asymptotically, $h_i/h_j \approx (\rho(\mathbf{x}_j)/\rho(\mathbf{x}_i))^{1/4}$; thus, in principle, one could control the distribution of generators to get equal distribution of the error by connecting the density function $\rho(\mathbf{x})$ to some priori or posteriori error estimates.

Thus, if the density function ρ is a constant on $\mathbf{S}^2$, then the CCVT generators will be "uniformly" distributed. Alternately, a non-constant choice for the density function provides an easy and systematic means for distributing points in a non-uniform manner; CCVT generators tend to accumulate in regions having relatively high values of ρ. However, unlike random sampling (with a suitably normalized ρ playing the role of

a probability distribution) for which the accumulation in regions having large ρ values occurs in a haphazard way, the accumulation of CCVT generators remains locally very regular. When applied to the numerical solution of PDEs, the density ρ may be related to the derivatives of the underlying solutions and thus provides a natural link between the distribution of generators and the need to efficiently resolve the PDE solutions.

5.2. Construction of CCVTs

Constructing a constrained mass centroid from its definition (5.1) is cumbersome. Fortunately, one can easily find a constrained mass centroid from the standard centroid obtained by viewing a subset of $\mathbf{S}^2$ as a subset of $\mathbb{R}^3$. To see how this is done, first note that the standard centroid of each V_i is defined by

$$\mathbf{x}_i^* = \frac{\int_{V_i} \mathbf{x}\rho(\mathbf{x})\,\mathrm{d}s(\mathbf{x})}{\int_{V_i} \rho(\mathbf{x})\,\mathrm{d}s(\mathbf{x})} \quad \text{for } i = 1,\ldots,n.$$

Clearly, $\mathbf{x}_i^*$ always falls inside the sphere $\mathbf{S}^2$. The connection between the constrained mass centroid $\mathbf{x}_i^{\mathrm{c}}$ and the standard mass centroid x_i^* is given in the following proposition.

Proposition 4. *Let $\mathbf{x}_i^{\mathrm{c}} \in \mathbf{S}^2$ and $\mathbf{x}_i^* \in \mathbb{R}^3$ denote the constrained and standard mass centroids of V_i, respectively. Then, $\mathbf{x}_i^* - \mathbf{x}_i^{\mathrm{c}}$ is a vector normal to surface $\mathbf{S}^2$ at $\mathbf{x}_i^{\mathrm{c}}$, i.e., $\mathbf{x}_i^{\mathrm{c}}$ is the projection of $\mathbf{x}_i^*$ onto $\mathbf{S}^2$ along the normal direction at $\mathbf{x}_i^{\mathrm{c}}$.*

Based on the projection property of Proposition 4, several deterministic and probabilistic algorithms have been proposed to determine the generators of constrained centroidal Voronoi tessellations on the sphere; see [6]. Parallel implementations of some probabilistic algorithms are discussed in [14].

We discuss one particular method known as *Lloyd's method* below since it was used to generate the constrained centroidal Voronoi meshes for the numerical experiments of Section 6.

Algorithm 1 (*Lloyd*'s method for CCVTs). Given a density function $\rho(\mathbf{x})$ defined for all $\mathbf{x} \in \mathbf{S}^2$ and a positive integer n,

0. select an initial set of n points $\{\mathbf{x}_i\}_{i=1}^k$ on $\mathbf{S}^2$, e.g., by random sampling or some other means;
1. construct the Voronoi sets $\{V_i\}_{i=1}^k$ of $\mathbf{S}^2$ associated with $\{\mathbf{x}_i\}_{i=1}^n$;
2. determine the constrained mass centroids of the Voronoi sets $\{V_i\}_{i=1}^n$; these constrained centroids form the new set of points $\{\mathbf{x}_i\}_{i=1}^n$;
3. if the new set of points meet some convergence criterion, terminate; otherwise, return to step 1.

Remark 3. Let $\mathbf{y}_1$ and $\mathbf{y}_2$ be the two end points of Γ_{ij}. If $a, b, f \in C^2(\mathbf{S}^2)$ and $\vec{\mathbf{v}} \in C^2(\mathbf{S}^2, \mathbb{R}^3)$, then we can use these following quadrature integration schemes:

$$\begin{cases} a_{ij} = \dfrac{1}{2}(a(\mathbf{y}_1) + a(\mathbf{y}_2)) \approx \dfrac{1}{m(\Gamma_{ij})} \displaystyle\int_{\Gamma_{ij}} a(\mathbf{x})\,\mathrm{d}\gamma(\mathbf{x}), \\ \beta_{ij} = \dfrac{m(\Gamma_{ij})}{2}(\vec{\mathbf{v}}\cdot\vec{\mathbf{n}}(\mathbf{y}_1) + \vec{\mathbf{v}}\cdot\vec{\mathbf{n}}(\mathbf{y}_2)) \approx \displaystyle\int_{\Gamma_{ij}} \vec{\mathbf{v}}(\mathbf{x})\cdot\vec{\mathbf{n}}_{\mathbf{x},V_i}\,\mathrm{d}\gamma(\mathbf{x}), \\ b_i = b(\mathbf{x}_i) \approx \dfrac{1}{m(V_i)} \displaystyle\int_{V_i} b(\mathbf{x})\,\mathrm{d}s(\mathbf{x}), \\ f_i = f(\mathbf{x}_i) \approx \dfrac{1}{m(V_i)} \displaystyle\int_{V_i} f(\mathbf{x})\,\mathrm{d}s(\mathbf{x}). \end{cases} \tag{5.2}$$

Then, Propositions 1 and 2 still hold if h is sufficiently small.

Remark 4. It is also worth noting that, due to the fact that $\mathbf{x}_i$ is the constrained centroid of V_i and Proposition 4, b_i and f_i in (5.2) have second-order truncation errors for a CCVT mesh. For general Voronoi meshes, they only have first-order truncation errors. Furthermore, for CCVT meshes, if $a, b, f \in C^2(\mathbf{S}^2)$ and $\vec{\mathbf{v}} \in C^2(\mathbf{S}^2, \mathbb{R}^3)$ and we use the approximations (5.2) in the finite volume scheme (3.5), the error estimate (4.12) will still hold.

6. Numerical experiments

In this section we present the results of some computational experiments involving CCVTs of the unit sphere. Voronoi meshes are generated from a set of generating points using the software package STRIPACK [18]. The generators of the CCVTs are determined using Lloyd's method (Algorithm 1).

6.1. Example CCVTs on the sphere

First, we illustrate CCVTs on the sphere and their desirable properties. In Fig. 2, we present CCVTs on the unit sphere for the *constant* density function $\rho(x_1, x_2, x_3) = 1$. This corresponds to a "uniform" distribution of generators. CCVTs for $n = 12$, 42, 162, 642, 2562, and 10 242, where n is the number of gener-

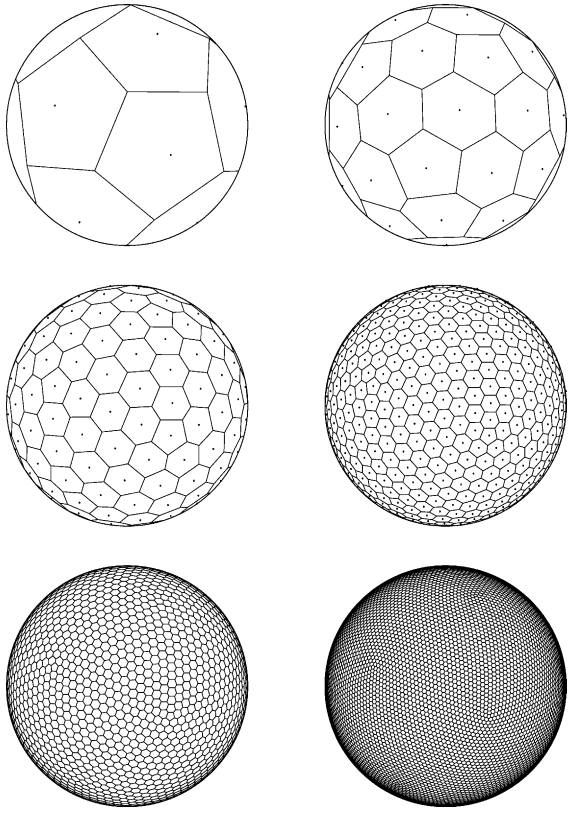

Fig. 2. Constrained centroidal Voronoi tessellations of the unit sphere for the constant density function $\rho(x_1, x_2, x_3) = 1$. Left-top: 12 generators; right-top: 42 generators; left-middle: 162 generators; right-middle: 642 generators; left-bottom: 2562 generators; right-bottom: 10 242 generators.

ators, are displayed. This sequence roughly corresponds to a sequence of refinements by successive halving of the grid size (quadrupling the number of points).

The sequence of grids illustrated in Fig. 2 was determined as follows. We started with the icosahedral mesh of 12 spherical pentagons; this mesh is, in fact, a CCVT mesh. (Other seed meshes may, of course, be used instead of the icosahedral mesh.) We then recursively determined a series of meshes through bisection, i.e., we added to the set of generators of a mesh the midpoints of the edges of the corresponding Delaunay triangulations. Except for the 42 point case, the members of this sequence of tessellations are not CCVTs. We then used each member of the bisection sequence of meshes as an initial condition for Lloyd's method (Algorithm 1) to produce the sequence of CCVT grids illustrated in Fig. 2.

Visually, from Fig. 2, the uniformity of the Voronoi cells is apparent; each CCVT displayed contains 12 spherical pentagons; the remaining Voronoi cells are spherical hexagons.

Of course, it is topologically impossible to tessellate the sphere exactly uniformly, e.g., into congruent spherical hexagons. If it were possible to tessellate the sphere into congruent spherical hexagons, it is easy to see that one would have $h\sqrt{n} \approx \sqrt{8\pi\sqrt{3}/9} \approx 2.2$ when n is large. Thus, we can use h as an indicator of the uniformity of point distributions on the sphere. The second row of Table 1 lists the values of the mesh norm h for the different values of the number of points n. We see that for CCVTs, h is indeed very close to the ideal value of $2.2/\sqrt{n}$.

Another measure of the regularity of a mesh is provided by σ which is defined by (2.2). The third row of Table 1 lists the values of σ for the different values of the number of points n. We see that, for CCVTs, σ is greater than 0.76 for all the values of n listed.

The results given in Table 1 as well as a visual inspection of Fig. 2 verifies that constant density CCVTs of the sphere are virtually ideally uniform. In fact, we have compared CCVTs to several other "uniform" meshes on the sphere and have found, using the measures just discussed, CCVTs to be superior, i.e., to be "more uniform."

Next, in Fig. 3, we present CCVTs on the unit sphere for the *non-constant* density function

$$\rho(x_1, x_2, x_3) = (1 - x_3^2)^{1/4} \mathrm{e}^{-2.5(1-x_3)}. \tag{6.1}$$

This density function vanishes at the north and south poles but achieves larger values in the northern hemisphere than it does in the southern hemisphere. CCVTs for $n = 162$, 642, 2562, and 10 242 are displayed. For the non-uniform point distributions resulting from the density function (6.1), the 162 point CCVT mesh is determined using Algorithm 1 starting from 162 points that are randomly selected using the density function (suitably normalized) as a probability distribution. The CCVT meshes with a greater number of points are determined as for the uniform distributions, i.e., starting with the 162 point mesh, we determine initial conditions for Algorithm 1 by successively bisecting the edges of the Delaunay triangulations.

Note from Fig. 3 that corresponding to the larger values of the density in the northern hemisphere relative to the southern hemisphere that there are more points placed in the former than in the latter. Using a construction algorithm for CCVT meshes, e.g., Algorithm 1, this non-uniform placement of points is automatic once the density function is specified. In Table 2, the mesh norm h and the regularity measure σ are given for the different values of n. Since the grid is not uniform, one cannot, of course, expect the mesh

Table 1
The mesh norm h and the regularity measure σ vs. the number of points n for constrained centroidal Voronoi meshes corresponding to the constant density function $\rho(x_1, x_2, x_3) = 1$

n	12	42	162	642	2562	10 242
h	0.6524	0.3609	0.1793	0.0892	0.0456	0.0238
σ	0.8481	0.7711	0.7662	0.7720	0.7677	0.7713

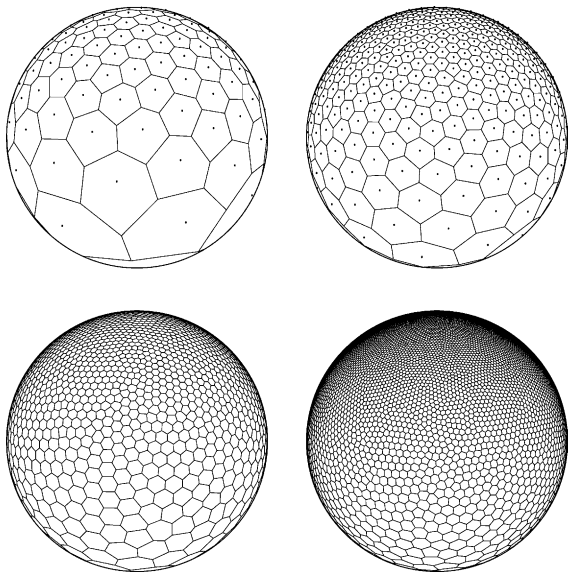

Fig. 3. Constrained centroidal Voronoi meshes on the surface of unit sphere for the non-constant density function $\rho(x_1,x_2,x_3)=(1-x_3^2)^{1/4}e^{-2.5(1-x_3)}$. Left-top: 162 generators; right-top: 642 generators; left-bottom: 2562 generators; right-bottom: 10 242 generators.

Table 2
The mesh norm h and the regularity measure σ vs. the number of points n for constrained centroidal Voronoi meshes corresponding to the density function $\rho(x_1,x_2,x_3)=(1-x_3^2)^{1/4}e^{-2.5(1-x_3)}$

n	162	642	2562	10 242
h	0.6186	0.3835	0.2194	0.1356
σ	0.3674	0.5183	0.5916	0.5980

norm h to be close to its ideal uniform value of about $2.2/\sqrt{n}$. However, we can still examine the regularity measure σ to measure the local regularity of the mesh. From Table 2, we see that as n increases, σ also increases and its value is not too far from that for the "uniform" mesh of Table 1. This and the visual evidence provided by Fig. 3 indeed show that CCVT meshes, even for non-uniform point distributions, are locally very regular.

The density function (6.1) is smoothly varying over the unit sphere and, not surprisingly, the resulting CCVT mesh also has cell sizes that vary smoothly. In some applications, one wants to have local refinement in the sense that one wishes to patch together two "uniform" grids with different cell sizes. The joining of the two disparate grids is often problematical. However, through a judicious choice for the density function that defines the point distribution for a CCVT grid, the transition from one grid to a locally refined grid can not only be systematically effected, but the resulting grids, at least visually, have very nice properties.

To illustrate these points, consider, on the unit sphere, the density function

$$\rho(x_1,x_2,x_3)=\begin{cases}1 & \text{if } d(\mathbf{x},\mathbf{x}_0)\leqslant 0.5\\ \max\{e^{-20(d(\mathbf{x},\mathbf{x}_0)-0.5)},0.05\} & \text{otherwise}\end{cases}\quad \text{with } \mathbf{x}_0=(1,0,0), \tag{6.2}$$

where $d(\cdot,\cdot)$ denotes the geodesic distance. Note that $\mathbf{x}_0$ is a point on the equator. In a geodesic circle centered at $\mathbf{x}_0$ and having radius 0.5, the value of the density function (6.2) is 20 times greater than its value

away from that circle. The exponential term in (6.2) effects a smooth transition between the two values (1 and 0.05) that the density function takes on most of the unit sphere. Since higher values of the density result in a closer spacing of points, we see that for the density function (6.2) the desired area of local refinement is the circle centered at $\mathbf{x}_0$. There is, of course, little difficulty encountered in defining density functions for other types of regions, e.g., rectangles, of local refinement.

In Fig. 4, we present CCVTs on the unit sphere for the *non-constant* density function (6.2). CCVTs for $n = 162$, 642, 2562, and 10 242 are displayed. In Table 3, the mesh norm h and the regularity measure σ are given for the different values of n. Again, one cannot expect the mesh norm h to be close to its ideal uniform value of about $2.2/\sqrt{n}$. However, the regularity measure σ again increases with n and achieves respectable values that indicate, as does a visual inspection of Fig. 4, that the CCVT meshes for the density function (6.2) are indeed locally quite uniform. Moreover, the transition between the two different "uniform" meshes is effected smoothly.

Remark 5. The properties of CCVTs discussed in this section also imply that they (or, more precisely, their dual Delaunay triangulations) are also very well suited in other settings such as piecewise polynomial interpolation on the sphere and for finite element discretizations of partial differential equations posed on a sphere.

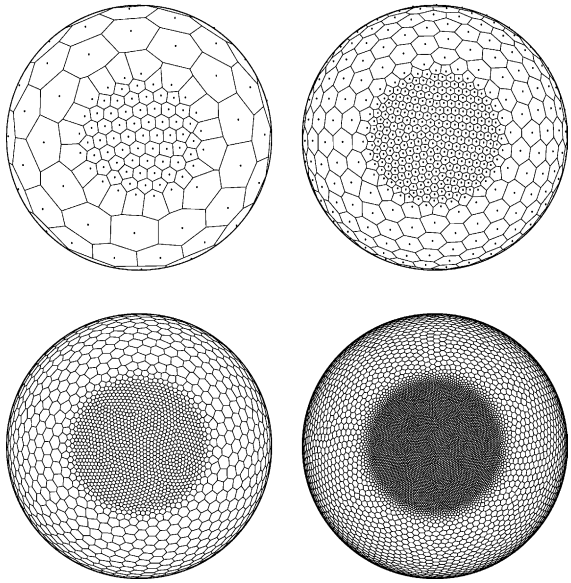

Fig. 4. Constrained centroidal Voronoi meshes on the surface of unit sphere for the piecewise constant density function $\rho(x_1, x_2, x_3)$ defined in (6.2). Left-top: 162 generators; right-top: 642 generators; left-bottom: 2562 generators; right-bottom: 10 242 generators.

Table 3
The mesh norm h and the regularity measure σ vs. the number of points n for constrained centroidal Voronoi meshes corresponding to the density function (6.2)

n	162	642	2562	10 242
h	0.2425	0.1250	0.0619	0.0348
σ	0.1891	0.3024	0.3958	0.5201

6.2. Experiments with the finite volume scheme

In order to easily construct exact solutions of the model problem (1.1), we rewrite that equation in the spherical coordinate system

$$\mathbf{x} = (r\sin\phi\cos\theta, r\sin\phi\sin\theta, r\cos\phi) \quad \text{for } \phi \in [0,\pi] \text{ and } \theta \in [0,2\pi).$$

Since on $\mathbf{S}^2$ u only depends on ϕ and θ, the component of $\vec{\mathbf{v}}$ in the r-direction has no effect on the solution of (1.1); thus, after introducing spherical coordinates, that component can be ignored. Thus, we can suppose that $\vec{\mathbf{v}}(\phi,\theta) = (v_1(\phi,\theta), v_2(\phi,\theta))$, where v_1 and v_2 are the (orthogonal) components of $\vec{\mathbf{v}}$ in the ϕ and θ directions, respectively, on the tangential surface of $\mathbf{S}^2$ at $\mathbf{x}$. We also have that

$$\nabla_s u(\phi,\theta) = \left(\frac{1}{r}\frac{\partial u}{\partial\phi}, \frac{1}{r\sin\phi}\frac{\partial u}{\partial\theta}\right)$$

and

$$\nabla_s \cdot \vec{\mathbf{v}}(\phi,\theta) = \frac{1}{r\sin\phi}\left(\frac{\partial}{\partial\phi}(v_1\sin\phi) + \frac{\partial v_2}{\partial\theta}\right).$$

For our first example, we choose the exact solution

$$u(\phi,\theta) = \sin^2\phi\cos^2\theta \tag{6.3}$$

and study three different model problems whose data are given in Table 4.

Approximate solutions were obtained using the finite volume scheme (3.5) and the uniformly distributed constrained centroidal Voronoi meshes of Fig. 2 and Table 1 which were based on the constant density function $\rho(x_1,x_2,x_3) = 1$. In Table 5, errors in the approximate solution vs. the number of generators are given. First, note that for the no convection case (Problem I), the error measured in the $\|\cdot\|_{1,\mathscr{W}}$ norm is indeed of $O(h)$, i.e., having of the grid size results in a halving of the error. This is in agreement with Theorem 1. The computational results for Problem I also indicate that the error measured in the $\|\cdot\|_{0,\mathscr{W}}$ norm is of second order, i.e., it is $O(h^2)$, and measured in the $\|\cdot\|_{L^\infty(\mathbf{S}^2)}$ is somewhere between first and second order. (Recall that there are no existing analytical results for these two cases in the literature, though it is possible to make a more refined analysis of the L^2 error that provides a theoretical confirmation of the experimental observation. It turns out that the rigorous justification of the $O(h^2)$ error in the L^2 norm depends crucially on the properties of the CCVT grid; details are to be presented in a forthcoming paper [7].) The behavior of the errors for the diffusion dominated case (Problem II) is similar. For the convection-dominated case (Problem III), the behavior of the error is erratic for relatively coarse meshes; for the finer meshes listed in Table 4, the behavior is similar to that for the other two problems, at least with respect to the $\|\cdot\|_{1,\mathscr{W}}$ and $\|\cdot\|_{0,\mathscr{W}}$ norms. All of these observations are in complete agreement with known results about finite volume schemes for planar regions; see, e.g., [16].

For the second example, the exact solution of (1.1) is chosen to be

$$u(\phi,\theta) = \mathrm{e}^{-5(1-\cos\phi)} = \mathrm{e}^{-5(1-x_3)}. \tag{6.4}$$

Table 4
Data for three model problems

		$a(\phi,\theta)$	$v_1(\phi,\theta)$	$v_2(\phi,\theta)$	$b(\phi,\theta)$
I	No convection	1	0	0	1
II	Diffusion dominated	$2+\sin^2\theta$	$\sin\phi/4$	$\sin\theta/4$	2
III	Convection dominated	0.05	$1+\sin\phi$	$1+\sin\theta$	$3.0+\sin^2\phi$

Table 5
Errors in the finite volume solution approximation for the three examples with exact solution (6.3) vs. the number of points n using constrained centroidal Voronoi meshes corresponding to the constant density function $\rho(x_1, x_2, x_3) = 1$

n		$\|e^h\|_{L^\infty(\mathbf{S}^2)}$	$\|e^h\|_{0,\mathscr{W}}$	$\|e^h\|_{1,\mathscr{W}}$
12	I	5.302E−02	1.181E−01	3.342E−01
	II	6.340E−02	1.550E−01	3.667E−01
	III	2.996E−01	4.163E−01	7.746E−01
42	I	1.446E−02	2.706E−02	8.304E−02
	II	2.022E−02	3.254E−02	1.171E−01
	III	2.524E−01	1.981E−01	6.411E−01
162	I	3.751E−03	6.427E−03	4.804E−02
	II	5.761E−03	8.152E−02	5.821E−02
	III	1.108E−01	5.676E−02	1.664E−01
642	I	9.561E−04	1.564E−03	2.232E−02
	II	1.941E−03	2.150E−03	2.832E−02
	III	7.171E−02	1.385E−02	8.392E−02
2562	I	2.461E−04	4.018E−04	1.175E−02
	II	5.261E−04	5.009E−04	1.469E−02
	III	2.094E−02	3.229E−03	4.367E−02
10 242	I	5.722E−05	9.393E−05	5.172E−03
	II	1.488E−04	9.905E−05	7.847E−03
	III	6.847E−03	7.597E−04	2.147E−02

Table 6
Errors in the finite volume solution approximation for the three examples with exact solution (6.4) vs. the number of points n using constrained centroidal Voronoi meshes corresponding to the constant density function $\rho(x_1, x_2, x_3) = 1$ and non-constant density function $\rho(x_1, x_2, x_3) = (1 - x_3^2)^{1/4} e^{-2.5(1-x_3)}$

n		$\rho(x_1, x_2, x_3)$					
		1			$(1 - x_3^2)^{1/4} e^{-2.5(1-x_3)}$		
		$\|e^h\|_{L^\infty(\mathbf{S}^2)}$	$\|e^h\|_{0,\mathscr{W}}$	$\|e^h\|_{1,\mathscr{W}}$	$\|e^h\|_{L^\infty(\mathbf{S}^2)}$	$\|e^h\|_{0,\mathscr{W}}$	$\|e^h\|_{1,\mathscr{W}}$
162	I	2.612E−03	4.117E−03	1.862E−02	8.334E−03	8.555E−03	1.436E−02
	II	5.345E−02	1.337E−02	8.851E−02	2.178E−02	1.429E−02	1.266E−01
	III	4.480E−01	9.025E−02	3.539E−01	4.405E−01	1.115E−01	4.516E−01
642	I	6.579E−04	1.001E−03	1.035E−02	1.749E−03	2.232E−03	7.655E−03
	II	3.571E−02	5.249E−03	4.449E−02	4.273E−03	3.282E−03	4.478E−02
	III	2.445E−01	5.534E−02	2.852E−01	1.939E−01	4.376E−02	2.411E−01
2562	I	2.117E−04	2.532E−04	5.267E−03	5.112E−04	5.953E−04	3.123E−03
	II	2.142E−03	1.732E−03	2.533E−02	1.222E−03	1.181E−03	2.552E−02
	III	2.242E−01	2.734E−02	2.222E−01	1.683E−01	1.524E−02	1.538E−01
10 242	I	1.055E−04	6.324E−05	2.643E−03	9.001E−05	1.409E−04	1.411E−03
	II	1.533E−03	8.349E−04	1.621E−02	6.565E−04	2.663E−04	1.624E−02
	III	1.178E−01	1.460E−02	1.456E−01	1.349E−01	4.666E−03	8.843E−02

It is clear that u achieves its maximum 1 at the north pole. In Table 6, errors in the approximate solution vs. the number of generators are given for CCVT grids generated using the constant density function $\rho(x_1, x_2, x_3) = 1$ and the non-constant density function defined in (6.1); see Figs. 2 and 3, respectively. The density function of (6.1) was actually determined by setting $\rho(x_1, x_2, x_3) = |\nabla_s u|^{1/2}$, where u is the exact

solution given in (6.4). Non-uniform CCVT meshes generated using the density function (6.1) should be a little better suited (although certainly not optimal) for the exact solution (6.4) compared to the uniform CCVT meshes based on a constant density function. For the most part, this is borne out by the results given in Table 6.

7. Concluding remarks

This paper was devoted to the following goals.

- We developed and analyzed a Voronoi tessellation-based finite volume scheme for the discretization of PDEs on the sphere and proved, for a simple model problem, that the scheme is first-order accurate with respect to a mesh-dependent discrete first-derivative norm.
- We introduced and discussed the notion of CCVT meshes on the sphere and illustrated the high-quality uniform and non-uniform meshes that are included in this special class of Voronoi meshes.
- We used computational experiments to illustrate the performance of the CCVT meshes used in conjunction with the finite volume scheme for the solution of simple model PDEs on the sphere. The experiments showed, for example, that the CCVT based finite volume approximations are second-order accurate if errors are measure in discrete L^2 norms.

There are, of course, many issues still to be addressed and several interesting directions for further study. The finite volume scheme we studied needs to be developed further in the contexts of the convection-dominated case, systems of PDEs, and non-linear PDEs so that they are applicable to realistic PDEs posed on the sphere. The CCVT methodology can also be applied to finite element discretizations of PDEs on the sphere. It is possible that high-quality CCVT meshes, both uniform and non-uniform, can effect improvements in PDE solutions on the sphere. Furthermore, the density function which helps define CCVT meshes should be related to a posteriori error bounds so that perhaps effective adaptive gridding strategies can be defined. All of these issues will be addressed in future work.

References

[1] F. Aurenhammer, Voronoi diagrams—A survey of a fundamental geometric data structure, ACM Comput. Surv. 23 (1991) 345–405.
[2] J. Baumgaedner, P. Frederickson, Icosahedral discretization of the two-sphere, SIAM J. Numer. Anal. 22 (1985) 1107–1115.
[3] Z. Cai, On the finite volume element method, Numer. Math. 58 (1991) 713–735.
[4] Y. Coudière, T. Gallouët, R. Herbin, Discrete Sobolev inequalities and L^p error extimates for finite volume solutions of convection diffusion equations, Math. Model. Numer. Anal. 35 (2001) 767–778.
[5] Q. Du, V. Faber, M. Gunzburger, Centroidal Voronoi tessellations: applications and algorithms, SIAM Rev. 41 (1999) 637–676.
[6] Q. Du, M. Gunzburger, L. Ju, Constrained centroidal Voronoi tessellations on general surfaces, SIAM J. Sci. Comput. 24 (2003) 1488–1506.
[7] Q. Du, L. Ju, Finite volume methods on spheres and spherical centroidal Voronoi meshes, preprint, 2003.
[8] R. Ewing, R. Lazarov, P. Vassilevski, Local refinement techniques for elliptic problems on cell-centered grids I. Error analysis, Math. Comput. 56 (1991) 437–461.
[9] G. Dziuk, Finite elements for the Beltrami operator on arbitrary surfaces, in: S. Hildebrandt, R. Leis (Eds.), Partial Differential Equations and Calculus of Variations, Lecture Notes in Mathematics, vol. 1357, Springer, Berlin, 1988, pp. 142–155.
[10] T. Gallouët, R. Herbin, M. Vignal, Error estimates on the approximate finite volume solution of convection diffusion equations with general boundary conditions, SIAM J. Numer. Anal. 37 (2000) 1935–1972.
[11] E. Hebey, Sobolev Spaces on Riemannian Manifolds, Springer, Berlin, 1991.
[12] R. Herbin, An error estimate for a finite volume scheme for a diffusion–convection problem on a triangular mesh, Numer. Meth. PDE 11 (1995) 165–173.

[13] J. Heinrich, P. Hyakorn, O. Zienkiewicz, A. Mitchell, An "upwind" finite element scheme for two-dimensional convective transport equations, Int. J. Numer. Meth. Engrg. 11 (1977) 131–143.
[14] L. Ju, Q. Du, M. Gunzburger, Probabilistic methods for centroidal Voronoi tessellations and their parallel implementations, Paral. Comput. 28 (2002) 1477–1500.
[15] R. Lazarov, I. Mishev, P. Vassilevski, Finite volume methods for convection–diffusion problems, SIAM J. Numer. Anal. 33 (1996) 31–55.
[16] I. Mishev, Finite volume methods on Voronoi meshes, Numer. Meth. PDE 14 (1998) 193–212.
[17] J. Nĕcas, Les Méthodes Directes en Théorie des Équations Elliptiques, Masson, Paris, 1967.
[18] R. Renka, Algorithm 772. Stripack: Delaunay triangulation and Voronoi diagrams on the surface of a sphere, ACM Trans. Math. Soft. 23 (1997) 416–434.
[19] T. Schmidt, Box schemes on quadrilateral meshes, Computing 51 (1993) 271–292.
[20] J. Thomas, D. Trujillo, Finite volume variational formulation: application to domain decomposition methods, Contem. Math. 157 (1994) 127–132.
[21] R. Vanselow, Relations between FEM and FVM, in: F. Benkhaldoun, R. Vilsmerier (Eds.), Finite Volumes for Complex Applications: Problems and Perspectives, Hermes, Paris, 1996.
[22] P. Vassilevski, S. Petrova, R. Lazarov, Finite difference schemes on triangular cell-centered grids with local refinement, SIAM J. Sci. Stat. Comput. 13 (1992) 1287–1313.